

Copyright is owned by the Author of the thesis. Permission is given for a copy to be downloaded by an individual for the purpose of research and private study only. The thesis may not be reproduced elsewhere without the permission of the Author.

**CT MEASUREMENT OF THE MOTION AND  
INCLINATION ANGLES OF THE SACROILIAC  
JOINT IN GERMAN SHEPHERD DOGS WITH AND  
WITHOUT LUMBOSACRAL REGION PAIN, AND  
IN GREYHOUNDS**

A thesis presented in partial fulfilment of the requirements  
for the degree of

Master of Veterinary Science  
at Massey University, Manawatu,  
New Zealand.

**Fritha Saunders**

**2013**

## Abstract

**Objective** – To develop an *in vivo* method to measure inclination angles and motion of the sacroiliac joint using CT, in two performance dog breeds, of which only one (the German Shepherd dog) has a predilection for diseases that cause lumbosacral region pain. Correlations were assessed in German Shepherd dogs between the presence of lumbosacral region pain and changes in these variables.

**Animals** – The study was comprised of 10 working German Shepherd dogs and 12 racing Greyhounds without history or evidence of lumbosacral region pain or neurological abnormalities, and 6 German Shepherd dogs with histories and examination findings consistent with lumbosacral region pain.

**Procedures** – CT scans were performed in flexed, neutral and extended positions. Lines placed on flexed and extended volume rendered images were used to measure motion of the ilium relative to the sacrum. Inclination angles (joint angle from a reference line placed in the dorsal plane) of the synovial and ligamentous joint components were measured on transverse plane images at a cranial and caudal location. Coefficients of variance were calculated.

**Results** – Coefficients of intra-observer variance ranged from 0.17-2.45%. German Shepherd dogs without lumbosacral region pain had greater rotational motion, and a more sagittally aligned cranial synovial joint component than Greyhounds. German Shepherd dogs with lumbosacral region pain had more rotational motion and X-axis translational motion than German Shepherd dogs without pain.

**Conclusions and Clinical Relevance** – A new method for measuring the motion and inclination angles of the sacroiliac joint, using CT has been presented. Small amounts of sacroiliac joint motion may be consistent with buffering of high frequency vibrations. The breed differences found may be linked to the German Shepherd dog's predilection for lumbosacral region pain. Differences in sacroiliac joint motion between German Shepherd dogs with and without lumbosacral region pain may be related to the presence of pain. There may be a causative relationship between diseases of the lumbosacral junction and increased sacroiliac joint motion. Further studies are needed to assess the motion and inclination angle variables, and to investigate these hypotheses.

# **Preface**

This thesis explores the ranges of motion (rotational and translational), and the inclination angles, of the sacroiliac joint in two large, working dog breeds (German Shepherd dogs and Greyhounds). It assesses correlations between these variables in German Shepherd dogs with and without lumbosacral region pain.

Approval for the use of the dogs was obtained from the Massey University Animal Ethics Committee.

## **Acknowledgements**

I would like to extend my sincere thanks to my supervisors, Angela Hartman, Nick Cave, Erica Gee and Andrew Worth, for giving me the opportunity to delve into this area of research, and for guiding my explorations into the research process. I would like to express my gratitude for their support, guidance, encouragement and commitment to the project. Their belief in me has helped me to achieve wonderful things over the last year.

My special thanks to Karl Hartman and Janis Bridges for their work on this project, and for their continued help, patience and encouragement throughout the year. Their support and good humour were invaluable.

I would also like to thank Alex Davies for sharing his insights and ideas on this topic with me.

I would like to acknowledge the New Zealand Police Dog Section of the New Zealand Police, and Greyhound Racing New Zealand for the use of the dogs and their cooperation and assistance in the performance of this study.

# Table of Contents

Abstract .....	ii
Preface.....	iii
Acknowledgements .....	iv
Table of Contents .....	v
List of Figures .....	viii
List of Tables.....	xi
List of Equations .....	xii
Abbreviations .....	xiv
Chapter One: Literature Review .....	1
1.1. Proposed functions of the sacroiliac joint .....	1
1.2. Anatomy of the sacroiliac joint.....	1
1.3. Inclination angles of the sacroiliac joint .....	5
1.4. Motion of the sacroiliac joint.....	7
1.4.1. An <i>in vitro</i> technique to measure sacroiliac motion in dogs .....	7
1.4.2. Techniques to measure sacroiliac motion <i>in vivo</i> .....	7
1.4.2.1. Horses.....	7
1.4.2.2. Humans .....	9
1.4.3. Summary of <i>in vivo</i> motion methodologies .....	10
1.5. Mechanisms, and diagnosis of sacroiliac pain .....	12
1.5.1. History of sacroiliac pain in humans and horses .....	12
1.5.2. Innervation of the sacroiliac joint.....	12
1.5.3. Diagnosis of sacroiliac joint pain .....	13
1.5.3.1. Humans .....	13
1.5.3.2. Horses.....	14

1.5.3.3. Dogs .....	14
1.6. Evidence of degeneration of the sacroiliac joint .....	15
1.6.1. Dogs.....	15
1.7. Relationships between sacroiliac, lumbosacral and coxofemoral joints in dogs .....	18
1.8. Imaging of the sacroiliac joint .....	19
1.9. German Shepherd dogs: use as working dogs .....	23
1.10. Conclusion .....	23
1.11. Research questions and hypotheses .....	24
1.11.1. Research questions .....	24
1.11.2. Null Hypotheses .....	24
Thesis Outline .....	26
Chapter Two: Unaffected dog study .....	27
2.1. Introduction.....	27
2.2. Materials and methods .....	32
2.2.1.1. Breed selection .....	32
2.2.2. Dogs.....	32
2.2.3. CT scan procedure .....	33
2.2.4. Motion .....	36
2.2.4.1. Motion methodology development .....	36
2.2.4.2. Measurement performance.....	38
2.2.4.3. Range of motion calculations.....	41
2.2.4.4. Definitions.....	48
2.2.5. Inclination angles .....	49
2.2.5.1. Inclination angle methodology development.....	49

2.2.6. Measurement performance .....	54
2.2.7. Statistical analysis .....	55
2.3. Results.....	56
2.3.1. Study design .....	56
2.3.2. Method validation.....	57
2.3.3. Motion .....	57
2.3.4. Inclination angles .....	58
2.4. Discussion .....	60
2.5. Conclusion .....	64
Chapter Three: Affected dog study .....	66
3.1. Introduction.....	66
3.2. Materials and methods .....	67
3.2.1. Study group selection .....	67
3.2.2. Measurement methodologies.....	67
3.2.3. Statistical analysis .....	68
3.3. Results.....	69
3.3.1. Dogs.....	69
3.3.2. Motion .....	73
3.3.3. Inclination angles .....	75
3.4. Discussion .....	76
3.5. Conclusion .....	81
Chapter Four: Conclusions.....	83
References .....	86



## List of Figures

Figure 1-1 Images of the sacroiliac joints showing the crescent-shaped synovial joint component (S), and the ligamentous joint component (L). A) Volume rendered image of the left sacroiliac joint surface after removal of the left ilium from the image. B) A transverse slice image through the sacrum (Sa), ilia (Il) and sacroiliac joints.....	3
Figure 1-2 Transverse section through the sacrum and ilium showing ridges with complimentary depressions (arrows) in the sacroiliac joint.....	4
Figure 1-3 Transverse slice image through the equine sacrum and ilium showing the oblique orientation of the sacroiliac joint .....	4
Figure 1-4 Schematic representation of the measurements performed by Breit and Kunzel (2001) to determine the inclination angles of the sacrum. They measured the dorsal and ventral transverse diameters of the sacrum (double-headed arrows) and calculated the inclination angle ( $\alpha$ Sac) of the sacral wing i.e. the angle of the surface of the sacral wing with the sagittal (vertical) plane. A) Representation of a more oblique inclination angle. B) Representation of a more sagittal inclination angle .....	6
Figure 1-5 A technique used to measure motion between the ilia using computed tomography, where PSIS is the posterior superior iliac spine, and ASIS is the anterior superior iliac spine, from Bussey MD, Yanai T, Milburn P. (2004). A non-invasive technique for assessing innominate bone motion. <i>Clinical Biomechanics</i> 19(1), 87.....	11
Figure 1-6 Lateral radiograph of the lumbosacral spine, sacroiliac joint and pelvis. The sacroiliac joint lies between the ilia (star) and the sacrum (circled).....	20
Figure 1-7 Symmetrical ventrodorsal view of the pelvis displaying the left and right sacroiliac joints (circled) and the right ilium (star). Note the faeces within the rectum overlying the left sacroiliac joint.....	21
Figure 2-1 Measurements of the inclination angles of the synovial components (S) and the ligamentous components (L) of the sacroiliac joint at the caudal location measured from the reference line (R). 1) The inclination angle of the right caudal ligamentous component; 2) the inclination angle of the right caudal synovial component; 3) the	

inclination angle of the left caudal synovial component; 4) the inclination angle of the left caudal ligamentous component.....	30
Figure 2-2 A schematic representation of the inclination angles of the sacrum: A) representation of a more oblique inclination angle B) representation of a more sagittal inclination angle.....	31
Figure 2-3 Computed tomography positioning for the flexed position; lateral view.....	34
Figure 2-4 Computed tomography positioning for the extended position; lateral view .	35
Figure 2-5 Computed tomography positioning for the extended position; caudal view.	35
Figure 2-6 A volume rendered image was targeted until the midline of the sacrum was displayed. A line was placed along the ventral surface of the dorsal sacral lamina. ....	37
Figure 2-7 The rendered image was expanded until the ilium was again visualised overlying the sacrum, and a line was placed on the ilium. ....	37
Figure 2-8 Placement of the ilial and sacral lines on the volume rendered computed tomography images of the ilium and sacrum .....	40
Figure 2-9 Display image of the ilial and sacral lines upon which measurements were performed.....	40
Figure 2-10 Measurements performed on the ilial and sacral lines using ClearCanvas Workstation. An angle marker (dotted line) was placed over the ilial and sacral lines (solid black lines) to determine the angle (degrees) of their intersection point. Measurements were made of the distances (cm) from the intersection point to the cranial point of the sacral line ( $S_1$ ), the caudal point of the sacral line ( $S_2$ ), the cranial point of the ilial line ( $I_1$ ), and the caudal point of the ilial line ( $I_2$ ). The sacral line was set as the X-axis, with the Y-axis set perpendicular to the X-axis .....	41
Figure 2-11 Schematic diagram of the calculations performed to determine the coordinates of the pivot point of the flexed and extended ilial lines ( $X_p, Y_p$ ) relative to the origin (0,0).....	44
Figure 2-12 Schematic diagram of the calculations performed to determine the X-axis and Y-axis translational movement of the ilial line between flexion and extension .....	45

Figure 2-13 Schematic diagram to determine calculations to convert $X_1', Y_1'$ relative to the origin, for situations where the ilial and sacral lines fall between the origin and $X_p, Y_p$ (A), where the ilial and sacral lines both fall on the far side of $X_p, Y_p$ (B), and where the cranial and caudal points fall on either side of $X_p, Y_p$ (C) .....	47
Figure 2-14 Lines were placed along the sacroiliac joint space, and along the ventral surface of the sacrum, along a tangent to the left and right ventrolateral sacral edges. The location of osteophyte on the ventral sacrum in some dogs (arrow) which produced variability in marker location. ....	51
Figure 2-15 Lines were placed along the sacroiliac joint space, and along the dorsal surfaces of the wings of the sacrum. ....	52
Figure 2-16 The lowest points in the dorsal sacral laminae (arrows) were used to position a reference line. ....	53
Figure 2-17 Transverse section through the sacroiliac joints with two inclination angle markers on the right sacroiliac joint showing potential variation in placement of marker along the axis of the joint space. ....	54
Figure 2-18 Distribution of average rotational motion vs. weight in German Shepherd dogs and Greyhounds .....	62

## List of Tables

Table 2-1 Raw data averages for the rotational and translational motion variables in German Shepherd dogs (GSD) and Greyhounds (GH). These averages do not take into account the interaction between rotational motion and bodyweight which is described by the model estimate equations in Table 2-2.....	58
Table 2-2 Parameter estimates and their standard errors from a mixed-effects linear regression model of rotational motion and the inclination angle of the cranial synovial component of the sacroiliac joint in German Shepherd dogs (GSD) and Greyhounds (GH). .....	59
Table 3-1 History, orthopaedic examination, neurologic examination and CT scan findings of the German Shepherd dogs affected by lumbosacral region pain (LS = lumbosacral).....	70
Table 3-2 Average values and standard deviations for the rotational and translational motion variables in affected German Shepherd dogs and unaffected German Shepherd dogs (GSD = German Shepherd dog) .....	73
Table 3-3 Parameter estimates and their standard errors for the mixed effect linear models of rotational motion, X-axis translational motion and Y-axis translational motion in affected German Shepherd dogs and unaffected German Shepherd dogs (GSD = German Shepherd dog) .....	74
Table 3-4 Parameter estimates and their standard errors for the mixed effect linear models of the inclination angle of the caudal ligamentous component in affected German Shepherd dogs and unaffected German Shepherd dogs .....	76

## List of Equations

$(180 - \phi_F)$	Equation 1 .....	42
$(\phi_F - \phi_E)$	Equation 2 .....	42
$\frac{a}{\sin A} = \frac{b}{\sin B}$	Equation 3 .....	42
$\frac{d}{\sin(180 - \phi_F)} = \frac{ds}{\sin(\phi_F - \phi_E)}$	Equation 4 .....	42
$d \sin(\phi_F - \phi_E) = ds \sin(180 - \phi_F)$	Equation 5 .....	42
$d = \frac{ds \sin(180 - \phi_F)}{\sin(\phi_F - \phi_E)}$	Equation 6 .....	42
$X_p = d \cos \phi_E - ds$	Equation 7 .....	42
$Y_p = d \sin \phi_E$	Equation 8 .....	43
$r^2 = a^2 + b^2$	Equation 9 .....	43
$r^2 = dx_r^2 + dy_r^2$	Equation 10 .....	43
$dx_r = X_p - X_{IF}$	Equation 11 .....	43
$dy_r = Y_p - Y_{IF}$	Equation 12 .....	43
$r = \sqrt{dx_r^2 + dy_r^2}$	Equation 13 .....	43
$r = \sqrt{(X_p - X_{IF})^2 + (Y_p - Y_{IF})^2}$	Equation 14 .....	43
$X_1 = c \cdot \cos \phi_E$	Equation 15 .....	43
$Y_1 = c \cdot \sin \phi_E$	Equation 16 .....	43
$[(X_p \pm X_1), (Y_p \pm Y_1)]$	Equation 17 .....	46

$dx_1 = X_{11E} - X_1`$ Equation 18.....	46
$dy_1 = Y_{11E} - Y_1`$ Equation 19.....	46

## Abbreviations

<b>CT</b>	Computed tomography
<b>GSD</b>	German Shepherd dog
<b>GH</b>	Greyhound dog
<b>MRI</b>	Magnetic resonance imaging
<b>SIJ</b>	Sacroiliac joint

# **Chapter One: Literature Review**

## **1.1. Proposed functions of the sacroiliac joint**

Many functions have been proposed for the sacroiliac joint (SIJ), and it is likely that the role of the joint is complex. Due to its location in the pelvic girdle, it is probable that the SIJ plays an important role in the transmission of propulsive forces from the hindlimbs to the vertebral column and trunk (Gembardt, 1974; Knaus et al., 2004), and resists the ventrally-directed gravitational forces of the trunk acting on the sacrum (Cook et al., 1996). Additional functions of the SIJ that have been proposed include buffering of ground impact forces (Brooke, 1924; Al-Khayer and Grevitt, 2007), moderation of pelvic torsion created by asymmetrical gait (Bogduk, 2005), and absorption of shearing forces produced between the ilium and sacrum during locomotion (Dontigny, 1985). The SIJ may also play a role in controlling and regulating posture (Indahl et al., 1999). It may be that there needs to be a trade-off between joint rigidity for force transmission and flexibility for its role in buffering and absorbing forces.

## **1.2. Anatomy of the sacroiliac joint**

The canine SIJ is a closely opposed joint comprised of a ligamentous component and a synovial component (Gregory et al., 1986). The ligamentous component is located craniodorsally and centrally, and is comprised of collagen fibres separated by adipose tissue (Figure 1-1) (Gregory et al., 1986). In young animals, these collagen fibres insert onto the subchondral bone through a zone of fibrocartilage. In adult dogs, the fibrocartilage zone is usually ossified, but areas of cartilage may be present at the junction of the ligaments and bone; thought to be formed by metaplasia of aging collagen bundles (Gregory et al., 1986). The collagen fibres are oriented at an oblique angle to the joint surface and are at the greatest density in the centre of the joint. There are fibres that originate on the dorsal ilial surface of the joint and insert ventrally on the sacrum, and fibres that originate on the ventral ilial surface and insert dorsally on the sacroiliac joint surface (Gregory et al., 1986). This configuration is thought to suspend the sacrum between the ilia and prevent ventral dislocation of the sacrum due to



bodyweight. The crescent-shaped synovial component is located caudoventrally. Both the sacral and the ilial surfaces of the synovial component are comprised of hyaline cartilage of similar structure to articular cartilage present elsewhere in the body (Gregory et al., 1986).

Gregory et al. (1986) reported that the ilial and sacral surfaces of the SIJ are roughened, and have ridges and complimentary depressions on the opposing surfaces (Figure 1-2). Ridges and depressions have also been recorded on the surface of equine SIJs (Dalin and Jeffcott, 1986a) and on mature human SIJs (Vleeming et al., 1990a). Flat surfaces are susceptible to shearing (Snijders et al., 1993). Ridges and depressions were found in humans to increase the coefficient of friction between the joint surfaces (Vleeming et al., 1990b), thus increasing the stability of the joint (Vleeming et al., 1990b) and decreasing shearing (Cusi, 2010).

It is thought that compression on the joint surfaces aids the surface ridges and depressions in providing joint stability, and preventing shearing during the transmission of forces between the hindlimbs and vertebral column (Vleeming et al., 1990a; Cusi, 2010).

Sacroiliac joints are aligned relatively closely to the vertical plane in dogs (Breit and Kunzel, 2001; Breit et al., 2002) and pigs (Indahl et al., 1999), and are positioned between the upright, medial surfaces of the ilia (Figure 1-2). In horses (Dalin and Jeffcott, 1986a), the SIJs are oriented at around 30° to the horizontal plane, with the sacrum positioned below the ilial surfaces (Figure 1-3).

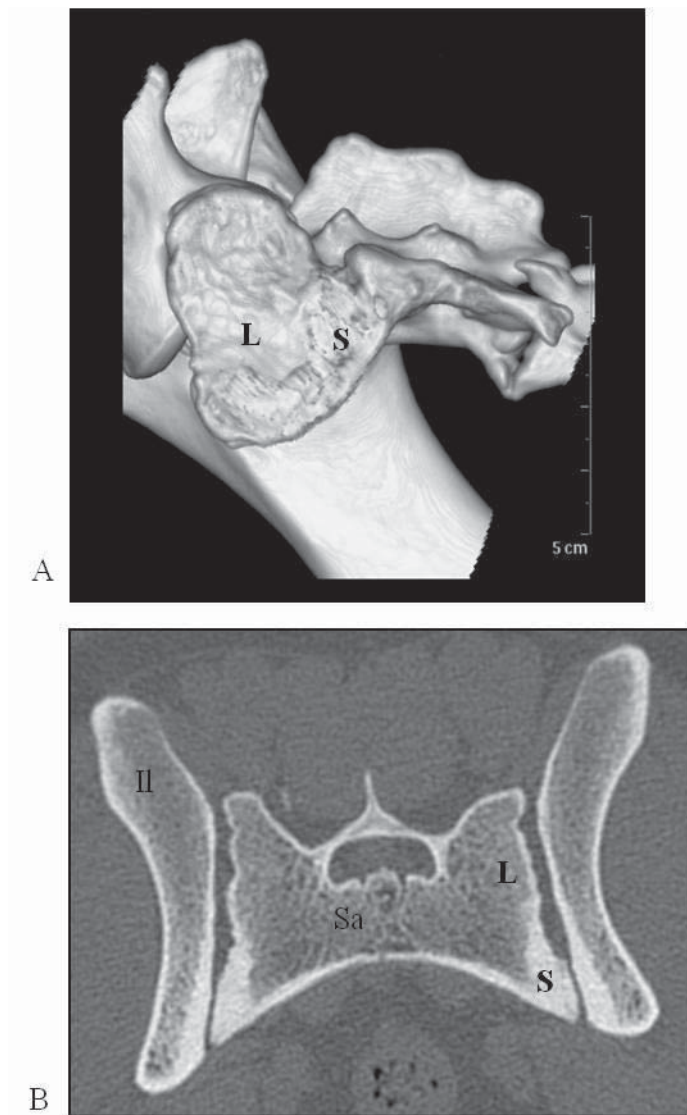


**Figure 1-1 Images of the sacroiliac joints showing the crescent-shaped synovial joint component (S), and the ligamentous joint component (L). A) Volume rendered image of the left sacroiliac joint surface after removal of the left ilium from the image. B) A transverse slice image through the sacrum (Sa), ilia (Il) and sacroiliac joints.**



**Figure 1-2 Transverse section through the sacrum and ilium showing ridges with complimentary depressions (arrows) in the sacroiliac joint.**

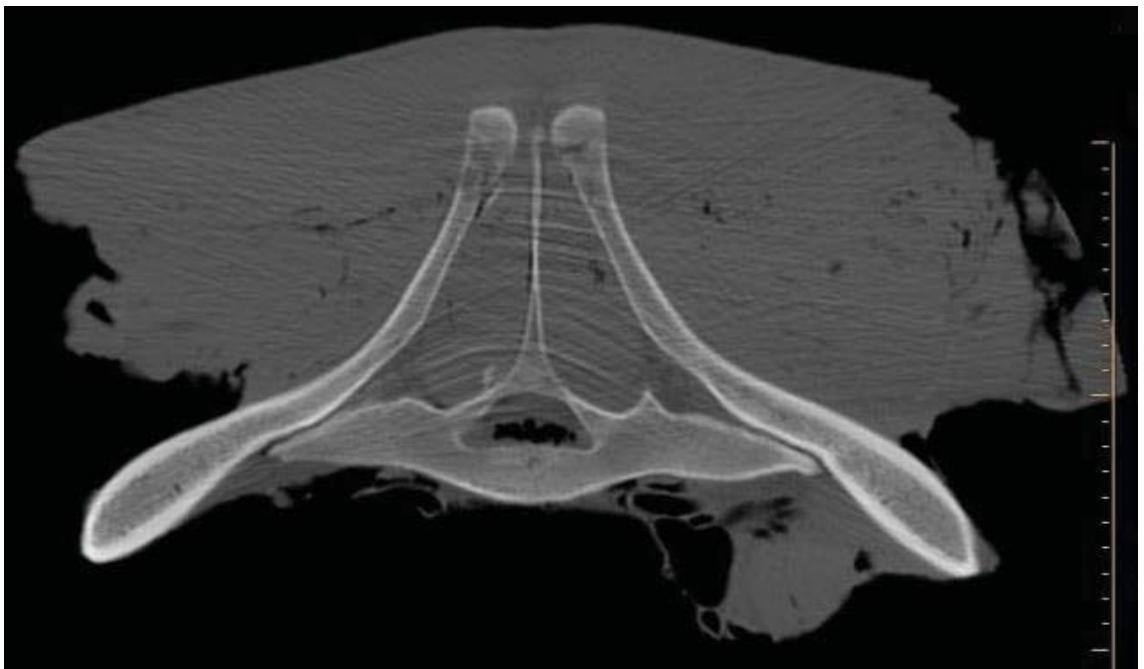


**Figure 1-3 Transverse slice image through the equine sacrum and ilium showing the oblique orientation of the sacroiliac joint**

### **1.3. Inclination angles of the sacroiliac joint**

Breit and Kunzel (2001) measured the transverse diameters of the dorsal and ventral surfaces of the sacrum and used these measurements to calculate the inclination angles of the surface of the sacral wing (called  $\alpha_{\text{Sac}}$ ) i.e. the degree that the surface of the sacral wing makes to the sagittal plane (Figure 1-4). These inclination angles were measured on macerated cadavers, and on symmetrical ventrodorsal radiographs of the canine pelvis. On ventrodorsal radiographs, the dorsal and ventral margins of the sacral wings were identified and used to measure the dorsal and ventral transverse diameters of the sacrum.

It has been proposed that the transmission of weight is affected by the inclination angle of the SIJ, which may therefore determine the loading capacity of the joint (Breit and Kunzel, 2001).

German Shepherd dogs (GSDs) were found by Breit et al. (2002) to have the most sagittally aligned SIJ of the breeds assessed. Furthermore, small breed dogs had more oblique (i.e. less sagittal) orientation of their SIJs, while large breed dogs tended to have SIJs closer to the sagittal plane (Breit and Kunzel, 2001). It may be that varying SIJ inclination angles have some relationship to differences in gait and spine flexibility, or body mass.

Breit and Kunzel (2001) also measured the craniocaudal (horizontal) inclination of the sacral wings in cadavers i.e. the degree to which the cranial width of the sacrum is wider than the caudal sacral width ( $\beta_{\text{Sac}}$ ). The importance of this measurement was purported to be in limiting craniocaudal translation of the sacrum relative to the ilium, where higher  $\beta_{\text{Sac}}$  angles were seen in 'wedge-shaped' sacra. Additionally, when the sacral contact surface was concave, the depth of the concavity was measured. The concavity was thought to help in limiting craniocaudal translation. The area of the sacroiliac contact surface was estimated from measurements of the height, and the craniocaudal extension of the sacral wing, assuming an elliptical shape of the contact area.

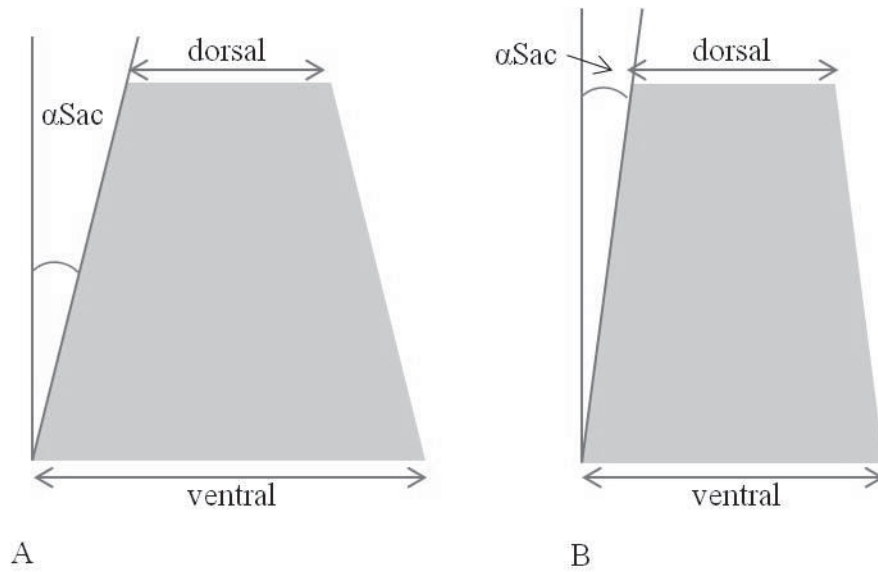


**Figure 1-4 Schematic representation of the measurements performed by Breit and Kunzel (2001) to determine the inclination angles of the sacrum. They measured the dorsal and ventral transverse diameters of the sacrum (double-headed arrows) and calculated the inclination angle ( $\alpha_{\text{Sac}}$ ) of the sacral wing i.e. the angle of the surface of the sacral wing with the sagittal (vertical) plane. A) Representation of a more oblique inclination angle. B) Representation of a more sagittal inclination angle**

## 1.4. Motion of the sacroiliac joint

Only one paper has been published measuring the motion of the canine SIJ (Gregory et al., 1986). These authors utilised an *in vitro* method to measure SIJ motion. As this Masters project was aimed to develop an *in vivo* method for measuring SIJ motion, this section of the literature review will also focus on reviewing the *in vivo* methodologies that have been used to measure SIJ motion in horses and humans.

### 1.4.1. An *in vitro* technique to measure sacroiliac motion in dogs

Sacroiliac joint motion in dogs has been measured in cadaver pelvises following dissection of the soft tissues surrounding the pelvis and SIJ, retaining the periarticular and sacrotuberous ligaments (Gregory et al., 1986). Parallel Kirschner wires were longitudinally placed in the sacral canal and through the wing of ilium. A weight was suspended from the ischiatic tuberosities creating displacement of the ilia relative to the sacrum. The angle of displacement between the wires was recorded and measurements were repeated following sequential severance of the periarticular and sacrotuberous ligaments, and the ligamentous component of the joint. The median value of SIJ range of motion was 7° (4-13°). There was no difference in range of motion found between dogs aged less than 4 years old and dogs aged 4-10 years old, or between male and female dogs. After the ligamentous component of the joint was severed, all joints disarticulated. The amount of weight used to create displacement of the ilia was calculated at 25% of the dog's bodyweight, but this appears to have been an arbitrarily chosen value. It is possible that removal of the soft tissues surrounding the pelvis, and freezing of the specimens may alter the amount of motion the joint is capable of, as compared with *in vivo* conditions.

### 1.4.2. Techniques to measure sacroiliac motion *in vivo*

#### 1.4.2.1. *Horses*

*In vivo* motion of the SIJ in horses has been investigated using 3-dimensional orientation sensors which measured motion between the ilium and sacrum at the walk and trot (Goff et al., 2010). Motion was compared between sensors mounted on the skin and sensors mounted on pins inserted into the bones. Skin sensors were mounted by palpating and marking the bony prominences of the two tuber sacrale, and the

spinous process of S3, then fixating the skin markers in place using stretch tape. The bone pins were inserted under sedation, through a stab incision in the skin and soft tissues overlying the tuber sacrale, the spinous process of S3, and the spinous process of the last lumbar vertebra.

The amount of motion measured at the trot was significantly different between pin- and skin- mounted sensors, and there was poor correlation in the data between pin- and skin-mounted sensors. The skin mounted sensors had greater variation in data between measurements taken at the start of the study, and at the end of the study; this was thought to be due to movement of skin over the bony landmarks causing dislodgement of the tape. The authors felt that the skin-mounted sensors provided unacceptable levels of error. A study comparing motion between bone-mounted markers and skin-mounted markers in the femur, tibia and metatarsus of sheep found that as the depth of soft tissue overlying the bone increased, the errors associated with prediction of the bone position using the skin markers also increased (Taylor et al., 2005). Another study found that the total error attributable to skin displacement during measurement of motion of the vertebral column was 10-30% (Faber et al., 2001). They concluded that skin markers can be used to quantify the kinematics of the vertebral column although they do not represent true movements of the vertebral column.

A source of error associated with the pin-mounted sensors noted by Goff et al. (2010) was the distance of the bones the pins were inserted into, from the articular surfaces of the SIJ. They suggest that their data represents the orientation of the bony landmark at a given point in time, rather than the motion of the SIJ.

Ultrasonography has been used to document motion at the SIJ by measuring changes in the cross-sectional area of the dorsal part of the dorsal sacroiliac ligament during manual pressure onto the pelvis in a dorsoventral direction (Goff et al., 2006). The changes in cross-sectional area of the ligament during pressure were compared between horses affected by sacroiliac disease, and unaffected horses. It was suggested that horses with sacroiliac disease may have instability in the SIJ (Jeffcott et al., 1985). It was proposed that instability of the joint could lead to increased joint motion under dorsoventral manual pressure (Goff et al., 2006). It was thought that increased joint motion may cause lengthening of the dorsal sacroiliac ligament due to increased



distance between its bony attachments. This could cause a decreased cross-sectional area of the ligament.

It was found that the cross-sectional area of the ligament decreased under dorsoventral manual pressure, but no difference was found between affected and unaffected horses. This methodology provided indirect support for the presence of movement at the equine SIJ, but could not be used to quantify motion of the joint as the measurements did not show direction or amplitude of motion.

#### *1.4.2.2. Humans*

Stereophotogrammetry has been the most widely tested method used to measure *in vivo* motion of the SIJ in humans. Initially, roentgen (x-ray) stereophotogrammetry was utilised to measure motion between the ilia and the sacrum in patients with sacroiliac disease (Egund et al., 1978; Stureson et al., 1989). Tantalum balls were permanently inserted into the ilia and the sacrum. Radiographs were taken with the subject in various positions. Known coordinates of calibration markers were used to determine the coordinates of the tantalum markers. Movement of the markers between positions was then calculated.

This method was later adapted to plain-light stereophotogrammetry (Jacob and Kissling, 1995). Photography was used instead of radiography to reduce the radiation exposure involved with taking repeated radiographs. Additionally, K-wires were inserted percutaneously into the ilia and sacrum instead of tantalum balls, so that they could be removed following the study. In a study of healthy volunteers, average rotation of the ilium relative to the sacrum was found to be  $1.7^{\circ}$  and average translation was 0.7 mm.

More recently, a technique to measure motion between the ilia was reported and validated (Bussey et al., 2004). Motion was measured by palpating and digitising the right and left anterior superior iliac spine and the posterior iliac spine landmarks using a magnetic tracking device. CT scans were performed to validate the technique. The angular displacement of the ilia was measured from the angle formed between a line that passed between the left and right posterior superior iliac spines, and a line that passed between the posterior superior iliac spine and the ipsilateral anterior superior iliac spine (Figure 1-5). This method measured motion between the two ilia, rather than the motion between one ilium and the sacrum. The range of motion with one hip



stressed was 2.50-3.2°. The mean range of motion with both hips stressed was 1.24-1.7°.

#### 1.4.1. Summary of *in vivo* motion methodologies

The methodologies that have been previously reported for use in measuring the *in vivo* motion of the SIJ have either been invasive (such as implanting tantalum balls or K-wires into the patient) or are considered to be inaccurate techniques (such as the use of skin markers following palpation of landmarks). Invasive methods are not feasible in dogs because their temperament makes them unsuitable for awake procedures involving inserting pins and manipulating the limb for measurements. No reports have been published of *in vivo* techniques which are both non-invasive and accurate.

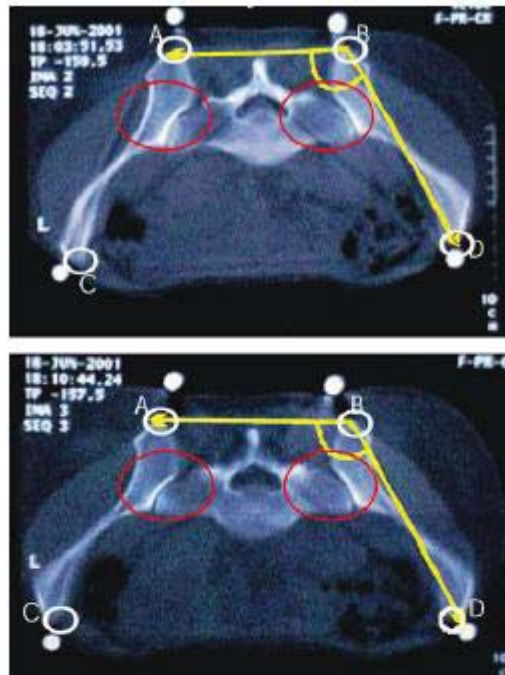


Fig. 3. CT scans of a cross-section through the palpated and digitized landmarks (PSIS and ASIS). In neutral (top) and stressed (bottom) the metallic beads, which were placed on the palpated and digitized point, appear white. These white markers represent the palpated and digitized surface landmarks and were used to align the CT scanner. These markers were not used in any subsequent analysis. When palpating the examiner attempted to palpate as deeply as possible, to “feel” the most prominent bony point of the PSIS and ASIS and this point was digitized. Measurements made from the CT image were taken from the most prominent bony point of the innominate bones themselves (marked with an O), thus A, B, C, D refer to the bony landmarks of the innominate bone. The sacroiliac joint has opened on both sides and the joint space is clearly visible within the circles. The vectors show how angle between innominate bones was calculated.

**Figure 1-5 A technique used to measure motion between the ilia using computed tomography, where PSIS is the posterior superior iliac spine, and ASIS is the anterior superior iliac spine, from Bussey MD, Yanai T, Milburn P. (2004). A non-invasive technique for assessing innominate bone motion. *Clinical Biomechanics* 19(1), 87**

## **1.5. Mechanisms, and diagnosis of sacroiliac pain**

### **1.5.1. History of sacroiliac pain in humans and horses**

The SIJ was considered as a site of pain in humans in the early twentieth century (Yeoman, 1928). The SIJ fell out of favour as a diagnosis of lower back pain in humans in the 1930s due to the discovery of intervertebral disc disease (Mixter and Ayer, 1935). In recent decades, the SIJ has regained attention in the literature as a site of pain in humans.

The earliest mentions of SIJ disease in horses were published in the mid 1970s (Jackson, 1975; Jeffcott, 1975; Rooney, 1977). At this time, there were conflicting opinions as to whether the SIJ was a site of pain. In the mid 1980s several studies were published describing the morphology and histology of the joint, and post mortem joint changes in horses suspected to have sacroiliac lesions (Dalin et al., 1985; Jeffcott et al., 1985; Dalin and Jeffcott, 1986a, 1986b). The SIJ has since remained a subject of interest in the equine literature.

It is unknown if the SIJ is a site of pain in dogs (Gregory et al., 1986; Knaus et al., 2003).

### **1.5.2. Innervation of the sacroiliac joint**

Innervation of the SIJ has been studied in several species including rats and humans, and is controversial. The innervation of the SIJ in rats was studied by denervating the dorsal and the ventral sides of the joint capsule and injecting a neural tracer into the synovial joint space (Murata et al., 2001). It was found that the SIJ is innervated by the dorsal root ganglia from L1 to S2, and that the dorsal and ventral components of the SIJ are innervated independently. The sensory nerve fibres which supply the dorsal portion of the joint are derived from the dorsal root ganglia of L4 to S2. The ventral portion of the joint is innervated by the dorsal root ganglia of L1 to L3. It is possible that neural tissue within the joint may be stimulated and cause pain when the joint undergoes abnormal loading and/or excessive movements (Knaus et al., 2004).

Calcitonin gene-related peptide (CGRP) and substance P immunoreactive nerve fibres have been detected in human SIJ cartilage, chondrocytes and in ligamentous tissue surrounding the cartilage and bone (Szadek et al., 2010). These structures may indicate

the presence of pain sensory fibres within the SIJ and provide support to the theory that articular structures of the SIJ can produce pain sensations.

Additionally, the successful intra-articular injection of local anaesthetics and steroids in the diagnosis and treatment of human patients, and peri-articular injections in equine patients with suspected SIJ pain makes it appear likely that the SIJ is a source of pain in these species (Dussault et al., 2000; Engeli and Haussler, 2012). One human study found that 66% of patients had a 50% decrease in pain upon intra-articular SIJ injection of local anaesthetic and corticosteroids, while 27% of patients had a decrease of 80% or more (Dussault et al., 2000). Marked gait improvement was observed in 100% of horses with suspected SIJ dysfunction following periarticular infusions (Dyson and Murray, 2003). In extrapolation, it would be logical that the SIJ is capable of causing pain in dogs.

### 1.5.3. Diagnosis of sacroiliac joint pain

#### *1.5.3.1. Humans*

The clinical signs of SIJ pain in humans mimic other causes of back pain making diagnosis difficult (Bernard and Cassidy, 1991). Clinical tests (such as pain provocation tests, motion demand tests and palpation tests) (Al-Khayer and Grevitt, 2007), pain referral zones and SIJ injections are used to aid in diagnosing SIJ pain. The validity and reliability of the clinical tests currently used is of concern as their success varies between performers, and they may also stress the lumbosacral and coxofemoral joints (Cattley et al., 2002). Pain referral patterns seen with SIJ pain are variable (Cattley et al., 2002) and may be similar to those seen in other causes of low back pain, such as that caused by lesions of the lumbosacral intervertebral disc, lumbar facet and coxofemoral joint (Bernard and Cassidy, 1991). The best test currently available for localisation of SIJ pain in humans is thought to be the use of intra-articular SIJ injections (Tuite, 2004), although this is not considered to be a gold-standard test by all authors (Cattley et al., 2002). Although performance of injections into the synovial joint component is technically challenging (Tuite, 2004) due to the complex anatomical structure of the joint, overlying structures limiting access to the joint, and the irregularities in the surface of the ligamentous component, a method using fluoroscopic needle guidance has been proposed which was reported to be straight-forward, accurate and fast (Dussault et al., 2000). Intra-articular joint injections can help in the diagnosis

of SIJ pain by either provoking the patient's symptoms through distension of the joint capsule, or via a decrease in pain following injection of local anaesthetic and steroids (Dussault et al., 2000). Although peri-articular joint blocks may be used therapeutically to treat suspected sacroiliac joint pain, dissemination of fluid to extra-articular structures prevents them from localising pain to the SIJ (Tuite, 2004).

#### *1.5.3.2. Horses*

Diagnosis of SIJ disease in horses is difficult due to non-specific clinical signs (Dyson and Murray, 2003) and the deep location of the joint (Jeffcott et al., 1985). Diagnosis is usually based on clinical signs and exclusion of other causes of poor performance (Engeli et al., 2004) with the support of local anaesthesia infiltration and nuclear scintigraphy (Dyson and Murray, 2003).

#### *1.5.3.3. Dogs*

Lumbosacral region pain in dogs is largely attributed to diseases of the lumbosacral vertebral facets, lumbosacral intervertebral disc and coxofemoral joint (Morgan et al., 2000). Physical manipulations designed to test for pain at the canine SIJ, such as the "thigh thrust test" and "shear tests", have not been validated (Edge-Hughes, 2007). A study has been performed to assess the accuracy of SIJ injections in canine cadavers (Jones et al., 2012). The authors found good accuracy for injection into the ligamentous component of the canine SIJ but only fair accuracy for injection into the synovial component. Sacroiliac joint injections have not been assessed *in vivo* in dogs, but Jones et al. (2012) suggest that this technique may be useful therapeutically for treating lumbosacral region pain, but is unlikely to be able to definitively localise pain to the SIJ due to diffusion of injected fluid throughout extraarticular soft tissues. As pain is currently unable to be localised to the SIJ, it is not known whether the SIJ is a site of pain in dogs.

## **1.6. Evidence of degeneration of the sacroiliac joint**

### **1.6.1. Dogs**

Several studies have reported the presence of degenerative changes in the canine SIJ (Gembardt, 1974; Gregory et al., 1986; Kunzel et al., 2002; Breit et al., 2003; Knaus et al., 2004). Histological findings of degeneration and erosion of the synovial cartilage, and osteophyte production around the joint have been noted (Gembardt, 1974; Gregory et al., 1986).

Small periarticular osteophytes have been reported surrounding the SIJ (Gregory et al., 1986). Gembardt (1974) noted that osteophytes were commonly present on the dorsomedial edge of the ilium and the ventrolateral edge of the sacrum. In support of these findings, Breit et al. (2003) and Knaus et al. (2004) reported osteophytes on the cranioventral margins of the synovial joint capsule on gross examination and on ventrodorsal radiographs. The osteophytes reported by Breit et al. (2003) were characterised by appearance of a new facet on the sacral surface, and/or a crest on the ilial surface. In moderate cases, the ilial crest grew ventrally around the sacral facet, embracing it. In severe cases there was complete ossification of the joint capsule; named ankylosis capularis ossea. In comparison to this, Knaus et al. (2004) reported that osteophytes were more common on the joint capsule attachment to the ilium. Bridging osteophytes were observed to occur at this location. Unilateral osteophytes were invariably associated with calcification of the collagen fibres in the contralateral joint (Breit et al., 2003).

Extrasynovial changes to the SIJ were more common than changes to the synovial component. Knaus et al. (2004) found that calcification of the ligamentous component of the joint was the most common lesion of the SIJs identified on ventrodorsal pelvic radiographs (63.4%). Calcification of the dorsal and/or ventral sacroiliac ligaments occurred with a lower prevalence (44%) and there was concurrent calcification of the ligamentous component in all but one joint. Complete calcification of the ligaments lead to ankylosis of the joint, even when the calcification was limited to individual fibres, or small bundles of fibres. Kunzel et al. (2002) found a radiographic prevalence of degenerative changes of the extra-synovial structures of the joint (in particular looking at exostoses, and mineralisation of the SIJ ligaments) of 73.3% of SIJs.

Synovial degenerative changes were present in 29.7% (Knaus et al., 2004) and 26.1% (Kunzel et al., 2002) of SIJs of canine patients that were radiographed for various reasons.

Gembardt (1974) reported on loss of congruency of the ridges and depressions on the opposing surfaces of the joint, which was thought to be due to laxity of the collagen fibres allowing ventral displacement of the sacrum relative to the ilium. Displacement of the joint surfaces relative to one another caused rubbing of opposing joint surfaces leading to cartilage damage. In areas, complete cartilage erosion had exposed the subchondral bone. Pannus tissue was present growing over areas of exposed subchondral bone and undergoing ossification (Gembardt, 1974; Gregory et al., 1986). Ossification of the pannus can lead to ankylosis of the joint (Gembardt, 1974; Gregory et al., 1986). Degenerative changes seen in the hyaline cartilage included thinning and fibrillation of the cartilage and proliferation of chondrocytes with necrosis of the cartilage matrix (Gembardt, 1974; Gregory et al., 1986). These changes are consistent with degenerative changes of synovial cartilage found elsewhere in the body (Gregory et al., 1986).

The age range of dogs in the study by Gregory et al. (1986) was from 3 months of age to 14 years old. Degenerative changes in the hyaline cartilage of the joints were seen microscopically in dogs as young as 5 months of age. The canine cadavers in the study by Breit et al. (2003) ranged from 1 day to 18 years old. In this study, gross and radiographic evidence of osteophyte was predominantly found in adult dogs, with only one dog under 1 year of age having degenerative changes. These degenerative changes mainly occurred in large and giant breed dogs versus small, or medium breed dogs ( $p < 0.001$ ).

Kunzel et al. (2002) suspected that the degenerative changes they observed on radiographs could have been caused by overloading of the joint, or by a congenital collagen defect leading to insufficiency of supporting connective tissue. This is in support of the theory suggested by Gregory et al. (1986) that degeneration of the SIJ was caused by overloading of the SIJ with resulting laxity in the supporting soft tissues (dorsal and ventral sacroiliac ligaments and the collagen fibres in the ligamentous component of the joint) leading to ventral displacement of the sacrum

No work has been done to assess the relationship between degenerative changes of the SIJs, such as production of periarticular osteophytes, and clinical signs of lumbosacral region pain in dogs. Although it is known that degenerative changes occur in the SIJ, the clinical significance of these degenerative changes is not known. Degenerative changes in human joints related to aging may not necessarily cause pain (Suri et al., 2007), but they may increase the expression of nociceptive structures in cartilage (Szadek et al., 2010). Although SIJ osteophytes have been imaged on canine radiographs, the prevalence of degenerative changes of the canine SIJ, such as osteophyte production, has not been assessed in dogs using cross-sectional modalities such as CT.



## **1.7. Relationships between sacroiliac, lumbosacral and coxofemoral joints in dogs**

The biomechanical relationships between the lumbosacral, coxofemoral and sacroiliac joints are not well understood. It has been suspected in the literature that dysfunction of the SIJ could either present solely as changes in the SIJ, or with concurrent changes in the adjacent lumbosacral and coxofemoral joints (Gregory et al., 1986; Kunzel et al., 2002; Knaus et al., 2003).

A post-mortem study of the vertebral columns of dogs, found that 28 out of 81 vertebral columns had exostoses or ankylosis at the lumbosacral joint. Ten of these dogs also had degenerative changes (such as osteophytes) at the SIJ (Gembardt, 1974). Another study found that degenerative changes of the canine SIJ noted on ventrodorsal pelvic radiographs were significantly associated with osteophyte production at the lumbosacral joint ( $p < 0.001$ ). In that study, 37% of dogs with lumbosacral spondylosis had osteophyte in the synovial component of the SIJ, and 84% had osteophyte in the extrasynovial joint components (Kunzel et al., 2002). Additionally, 56% of dogs with hip dysplasia had lumbosacral spondylosis, 26% had degenerative changes in the synovial component of the SIJ, and 80% had degenerative changes in the extrasynovial SIJ components (Kunzel et al., 2002). Kunzel et al. (2002) did not determine causality of the changes seen. The authors of both studies theorised that cumulative overloading may have played a role in the degeneration identified at these joints.

Although it has yet to be determined, it may be that SIJ degeneration could occur secondary to dysfunction of the lumbosacral or coxofemoral joints. Alternatively, it is possible that degenerative changes at the SIJ could alter the loading or function of the adjacent joints. The clinical significance of degenerative changes at the canine SIJ has not yet been assessed.

## **1.8. Imaging of the sacroiliac joint**

Radiography used to be the standard imaging modality used to image the SIJ (Murphey et al., 1991). With the advent of cross-sectional imaging modalities (CT and MRI), increased visualisation of the joint is possible.

Radiography produces 2-dimensional images using x-rays. Radiographic views used to image the canine SIJ include lateral projections (Figure 1-6) and ventrodorsal projections of the pelvis and lumbosacral spine (Figure 1-7). It has been proposed that ventrodorsal projections should include views with the sacrum at a centrally oriented position, and at an angled position (Breit et al., 2002; Crawford et al., 2003). Two major limitations of ventrodorsal radiographs are superimposition of the complex 3-dimensional anatomy of the SIJ, and the limited ability to distinguish tissues of the same opacity. The joint space does not lie in the sagittal plane in either the dorsoventral, or the craniocaudal directions. Thus, given the nature of joint obliquity to the standard dorsoventral and lateral planes, no aspect of the joint is truly sagittally aligned (Figure 1-6, Figure 1-7) (Knaus et al., 2003). Additionally, the irregularities of the joint surface overlap the joint space. This makes it difficult to project the x-ray beam through the joint space without superimposition of bone structures over the space. Finally, the ilium partially overlies the joint in ventrodorsal radiographs, and overlies the sacrum in lateral radiographs. These factors cumulate to make interpretation of the SIJ on radiographs difficult (Knaus et al., 2003). In one study, the dorsal and ventral outlines of the joint space were unable to be visualised in 23.3% of centrally positioned, symmetrical, ventrodorsal radiographs (Knaus et al., 2003). Interpretation ability is also limited if faeces are present within the rectum (Figure 1-7) (Crawford et al., 2003).

The advantages of radiography for analysis of the SIJ include cost-effective studies, the availability of equipment in most veterinary practices, the ability to perform many studies awake or under sedation, the low dose of radiation relative to CT, and the speed of the studies.

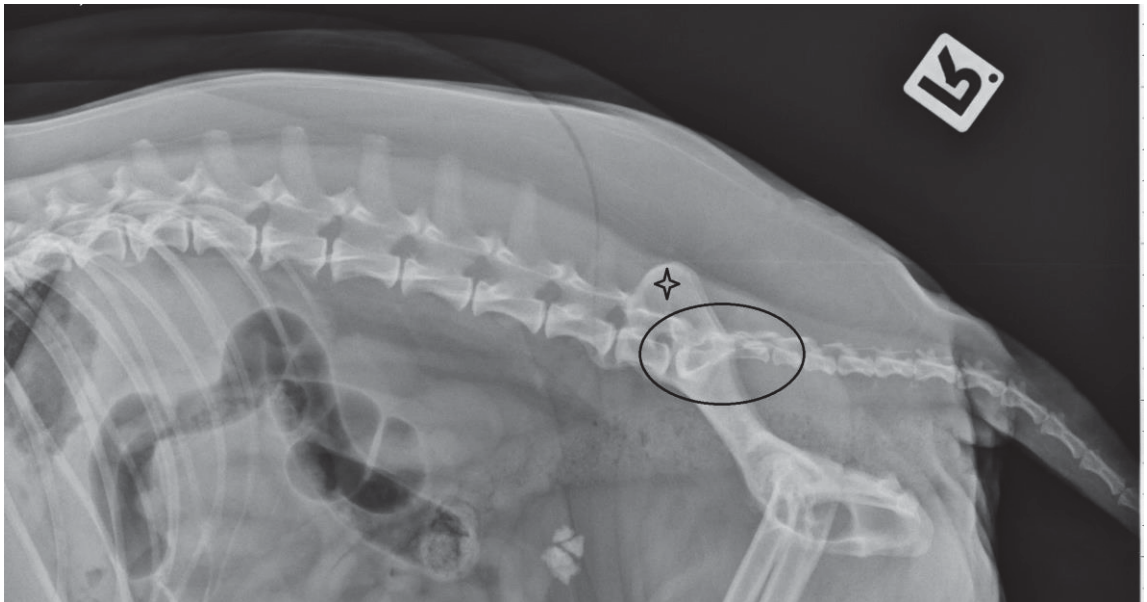


**Figure 1-6 Lateral radiograph of the lumbosacral spine, sacroiliac joint and pelvis. The sacroiliac joint lies between the ilia (star) and the sacrum (circled).**

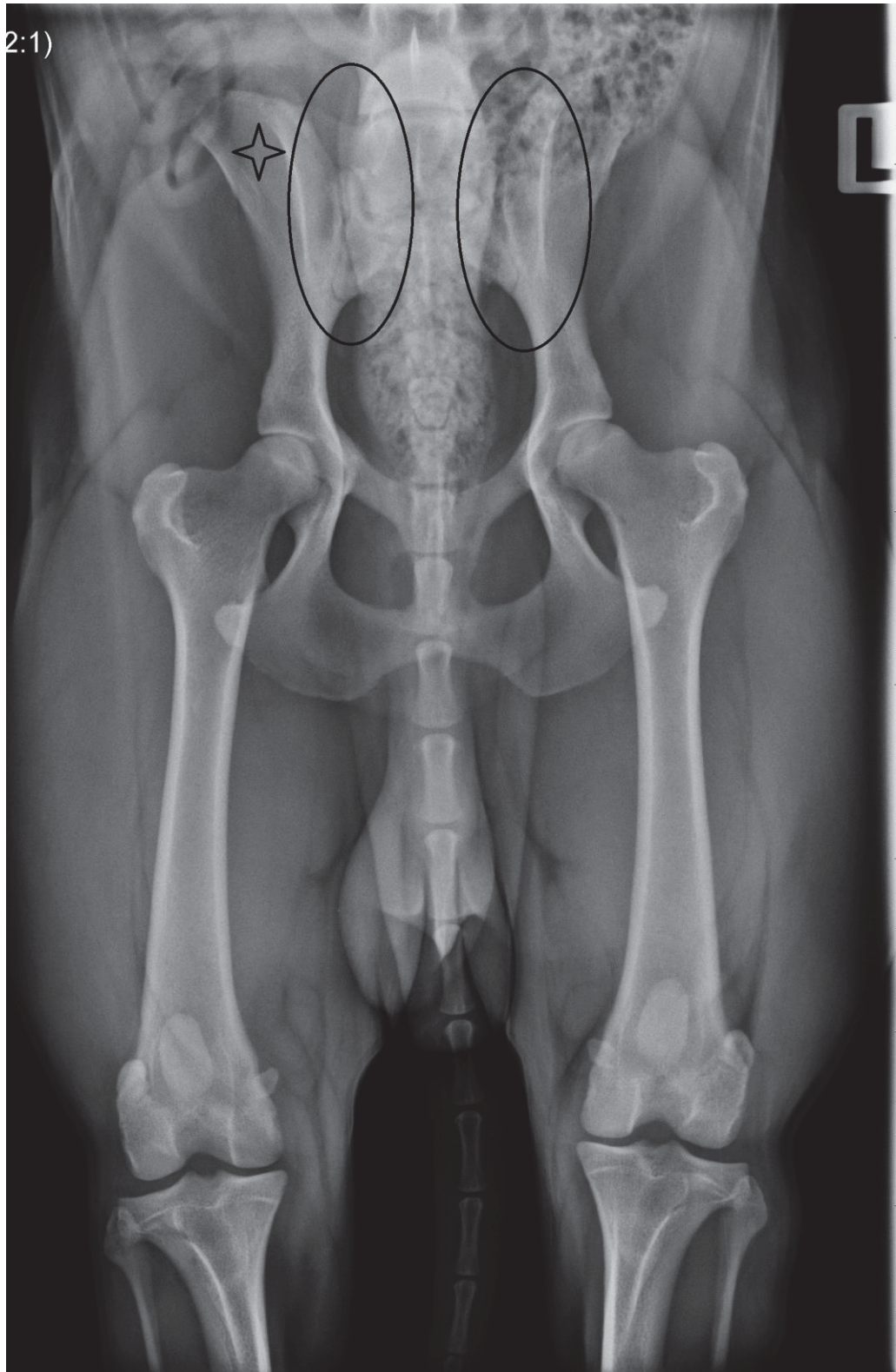


**Figure 1-7 Symmetrical ventrodorsal view of the pelvis displaying the left and right sacroiliac joints (circled) and the right ilium (star). Note the faeces within the rectum overlying the left sacroiliac joint.**

CT is superior to radiography for imaging the SIJ because the joint space can be directly visualised using cross-sectional slice images. In an anatomic investigation of the canine lumbosacral spine utilising CT, CT was found to be an effective means of visualising the SIJ in all dogs examined (Jones et al., 1995). Both components of the joint as well as the underlying subchondral bone were able to be clearly visualised. CT was found to be better than radiography at identifying traumatic lesions of the canine SIJ with less variation between readers and more definitive identifications made (Crawford et al., 2003). Sacroiliac joint narrowing, erosions and sclerosis of the human SIJ were clearly able to be identified by CT (Yu et al., 1998). CT was better than radiography at detecting erosions ( $p<0.001$ ) and sclerosis ( $p<0.01$ ), and better than MRI at detecting sclerosis ( $p<0.05$ ). It should however be noted that imaging findings are not always correlated to the painfulness of a joint (Dussault et al., 2000). Unlike MRI, CT cannot be used to visualise cartilage (Yu et al., 1998) without contrast arthrography being performed.

The advantages of CT as compared to radiographs include the ability to create cross-sectional slice images through the SIJ removing the effects of superimposition, the ability to create manipulable 3-dimensional (volume) rendered images, and the increased contrast resolution between tissues of different opacities and within osseous structures. The disadvantages of CT include the need for heavy sedation or general anaesthesia, higher cost than radiographs, high radiation dose, and limited ability to distinguish soft tissue structures as compared to MRI.

A reliable CT method has been proposed for detecting motion between the ilia *in vivo* (Bussey et al., 2004). Motion of one ilium relative to the other was measured using slice CT images, but no attempts have been made to directly measure *in vivo* motion between the ilium and sacrum in any species using CT.

The canine SIJ has been shown to be able to be clearly visualised using CT (Jones et al., 1995). CT has the ability to create slice images and reconstructions of the pelvis and vertebral column which remove the effects of superimposition seen on radiographs. Despite this, little work has been done on the canine SIJ using CT.

## 1.9. German Shepherd dogs: use as working dogs

German Shepherd dogs are acknowledged to have a breed predilection for diseases causing lumbosacral region pain (Schulman and Lippincott, 1988; Flückiger et al., 2006). German Shepherd dogs are commonly used as working police and military dogs (Moore et al., 2001; Evans et al., 2007). Nearly 50% of the military working dogs used by the US military between 2000 and 2004 were GSDs (Evans et al., 2007). Out of all the GSDs aged 5 years or older that were discharged from use during this time frame, 13% were discharged for “spinal cord disease and DJD”. Intense, repetitive motions performed by working dogs may have an impact on overloading the SIJ (Gembardt, 1974).

German Shepherd dogs are selected for use as general purpose dogs in the New Zealand Police Dog Section due to their size, temperament and trainability<sup>1</sup>. In 2012 there were 115 New Zealand Police Dog Handlers, with 90-95 dogs in service, and 10-15 dogs in training<sup>2</sup>. These dogs are socially and economically valuable animals, and lumbosacral region pain can be career limiting. The involvement of the SIJ in lumbosacral region pain is unknown.

## 1.10. Conclusion

The SIJ is a difficult joint to study due to its complex 3-dimensional anatomy and location of the joint in the body. The role of the joint has not been confirmed, but is likely to be multifactorial. Sacroiliac joint motion in the dog has been measured *in vitro*. *In vivo* methods for measuring SIJ motion have been developed in humans and horses, but no method has been developed as yet which is both non-invasive and accurate. Altered joint motion may lead to degeneration of the SIJ, but it is unknown in dogs what the normal *in vivo* motion of the SIJ is, and, whether increased or decreased motion causes lumbosacral region pain. Canine SIJ inclination angles have been measured on symmetrical ventrodorsal pelvic radiographs, and in cadavers. It has been

---

<sup>1</sup> New Zealand Police. (n.d.). *New Zealand Police Dog Unit* retrieved from <http://www.police.govt.nz/service/dogs>

<sup>2</sup> Inspector Brendon Gibson, New Zealand Police Dog Section, Personal Communication, March 2012



proposed that the transmission of weight is affected by the inclination angle of the SIJ, which may therefore determine the loading capacity of the joint.

CT can be used to visualise the canine SIJ, and the cross-sectional properties of CT make it likely to be a valuable tool in assessing this joint. CT has not been utilised to quantify the SIJ in dogs.

German Shepherd dogs are economically and socially valuable animals used frequently in military and police roles. These dogs are susceptible to lumbosacral region pain, which can be career limiting. The clinical significance of degenerative changes in the canine SIJ is unknown. Currently, it is not possible to localise lumbosacral region pain to the SIJ in dogs. As such, the involvement of the canine SIJ in lumbosacral region pain is unknown.

## **1.11. Research questions and hypotheses**

### **1.11.1. Research questions**

What is the intra-observer variability in the CT measurement of:

- The inclination angles of the SIJ?
- The ranges of motion of the SIJ?

Is there any difference in the inclination angles, and the amount of rotational, X-axis translational and Y-axis translational motion of the SIJ between:

- Working GSDs not currently affected by lumbosacral region pain compared to racing Greyhounds (GHs) not currently affected by lumbosacral region pain?
- Working GSDs not currently affected by lumbosacral region pain compared to working GSDs affected by lumbosacral region pain?

### **1.11.2. Null Hypotheses**

That there is no significant difference in the inclination angles and motion of the SIJ between:

- Working GSDs not currently affected by lumbosacral region pain compared to racing GHs not currently affected by lumbosacral region pain.
- Working GSDs not currently affected by lumbosacral region pain compared to working GSDs affected by lumbosacral region pain.

The alternative hypotheses are two-tailed hypotheses i.e. that there is a difference between the groups, without specifying in which group the variable is larger.



## **Thesis Outline**

This thesis describes the development of a method to measure SIJ motion and inclination angles using CT in German Shepherd dogs (GSDs) and Greyhounds without lumbosacral region pain (Chapter Two). This method was then applied to GSDs with lumbosacral region pain, as compared to GSDs without pain, as described in Chapter Three.

The contents of Chapter Two have been published in the American Journal of Veterinary Research, volume 74, issue 9, September 2013.

## **Chapter Two: Unaffected dog study**

### **2.1. Introduction**

The canine sacroiliac joint (SIJ) is a closely opposed joint composed of a ligamentous component, and a synovial component (Gregory et al., 1986). The ligamentous component is located craniodorsally and centrally, and is composed of fascicles of collagen fibers separated by adipose tissue. The synovial component is crescent shaped and located caudoventrally. It has been proposed that the SIJ needs to transmit propulsive forces from the pelvic limbs to the vertebral column and resist the weight of the torso, but it may play a role in the buffering of ground impact forces (Cook et al., 1996; Breit and Kunzel, 2001; Knaus et al., 2004; Al-Khayer and Grevitt, 2007). These roles may require a trade-off between the rigidity needed for force transmission and flexibility required for the joint to act as a buffer to high frequency motion being transmitted through this region.

Although controversial, the SIJ is recognised as a site of pain in humans (Maigne and Planchon, 2005) and horses (Jeffcott et al., 1985), but it is not known if the SIJ is a source of pain in dogs (Gregory et al., 1986; Knaus et al., 2003). The clinical signs of SIJ pain in humans mimic other causes of back pain (Bernard and Cassidy, 1991). Pain provocation tests for human SIJ dysfunction may not be specific for the SIJ as they also stress the lumbosacral and coxofemoral joints (Cattley et al., 2002). Dogs can suffer from lumbosacral region pain (Knaus et al., 2003), which is largely attributed to diseases of the lumbosacral vertebral facets, lumbosacral intervertebral disc and coxofemoral joint (Morgan et al., 2000). Physical manipulations designed to test for pain at the canine SIJ, such as the “thigh thrust test” and “shear tests”, have not been validated (Edge-Hughes, 2007). Therefore it is not known whether the SIJ is a site of pain in dogs. German Shepherd dogs (GSDs) are acknowledged to have a breed predilection for diseases causing lumbosacral region pain (Schulman and Lippincott, 1988). German Shepherd dogs are commonly used as working police and military dogs (Moore et al., 2001; Evans et al., 2007). These dogs are socially and economically valuable animals, and lumbosacral region pain can be career limiting.

Forces from the pelvic limbs are transmitted into the vertebral column through the coxofemoral joint, the SIJ, and the lumbosacral joint (Cook et al., 1996). It has been

proposed that overloading of the canine SIJ such as that caused by repetitive, intense activity or work, may lead to instability of the SIJ (Gembardt, 1974; Breit and Kunzel, 2001; Breit et al., 2002). Sacroiliac joint instability could lead to secondary joint disease and osteophyte production at the SIJ, which could in turn limit SIJ motion and transfer abnormal loading to the adjacent coxofemoral and lumbosacral joints (Gembardt, 1974). Therefore, it is possible that secondary joint disease of the SIJ in dogs could cause pain locally at the SIJ, or at adjacent structures (Gregory et al., 1986; Breit et al., 2003). Alternatively, degenerative changes in the SIJ could occur secondary to diseases of the lumbosacral junction and coxofemoral joint which alter loading of the SIJ (Knaus et al., 2003). It is important to understand what the normal biomechanics of the canine SIJ are before hypotheses can be drawn about sources of SIJ pain.

Motion of the canine SIJ has been measured in one cadaveric study which involved dissection of the soft tissues surrounding the SIJ, with retention of the periarticular and sacrotuberous ligaments, in which an average rotational motion of  $7^{\circ}$  ( $4\text{--}13^{\circ}$ ) was described (Gregory et al., 1986). No work has been done to assess *in vivo* motion in dogs. Studies analyzing *in vivo* motion in horses have utilised skin-mounted sensors (Taylor et al., 2005; Goff et al., 2010), bone marker implants (Goff et al., 2010), and indirect measurement through ultrasonographic examination of the dorsal sacroiliac ligament (Goff et al., 2006). *In vivo* motion studies in humans have been performed using roentgen stereophotogrammetry of tantalum implants (Sturesson et al., 1989), plain-light stereophotogrammetry of k-wire implants (Jacob and Kissling, 1995), and transcutaneous palpation and digitization of landmarks (Bussey et al., 2004). Computed tomography (CT) has previously been shown to be a reliable method of detecting motion *in vivo* (Bussey et al., 2004), however, to the author's knowledge, no attempts have been made to directly measure motion between the sacrum and ilium using CT in any species.

Inclination angles of the SIJ are defined as the angle of the axis of the joint relative to a dorsally positioned reference line, as measured on transverse plane images (Figure 2-1). The transmission of weight is affected by the inclination angle of the SIJ, which may therefore determine the loading capacity of the joint (Breit et al., 2002). The canine SIJ is aligned relatively closely to the sagittal axis (Breit et al., 2002). It is proposed that as the alignment of the SIJ nears the sagittal plane, the direction of loading forces are closer to being parallel with the joint surfaces than when the joint is more obliquely

aligned. This may mean that a more sagittal SIJ experiences more shearing forces than a more oblique joint (Figure 2-2). German Shepherd dogs were found to have the most sagittally aligned SIJ of the breeds assessed (Breit et al., 2002). Furthermore, it was found that small breed dogs had more oblique (i.e. less sagittal) orientation of their SIJs, while large breed dogs tended to have SIJs closer to the sagittal plane (Breit et al., 2002). It may be that varying SIJ inclination angles have some relationship to differences in gait or body mass. Sacroiliac joint inclination angles have not been measured in active working dogs.

Sacroiliac joint inclination angles have been previously measured in canine cadavers and on symmetrical ventrodorsal pelvic radiographs (Breit et al., 2002). Radiography involves visualisation of the sacral wings rather than direct visualisation of the joint space. Visualisation of the outlines of the joint space was found to be inconsistent in radiographic projections of the canine pelvis (Knaus et al., 2003). Although the SIJ has been successfully imaged by CT, it has not yet been used to quantify the inclination angles of the joint (Jones et al., 1995).

This study was designed to develop a new, non-invasive *in vivo* method to measure the motion and inclination angles of the SIJ using CT. Two large, performance dog breeds were selected for this study, of which only one, (the GSD), is predisposed to caudal back pain. It was hypothesised that motion and inclination angles of the SIJ would be able to be measured using this CT method, and that there would be differences in the ranges of motion, and the inclination angles of the SIJ between GSDs and Greyhounds (GHs).

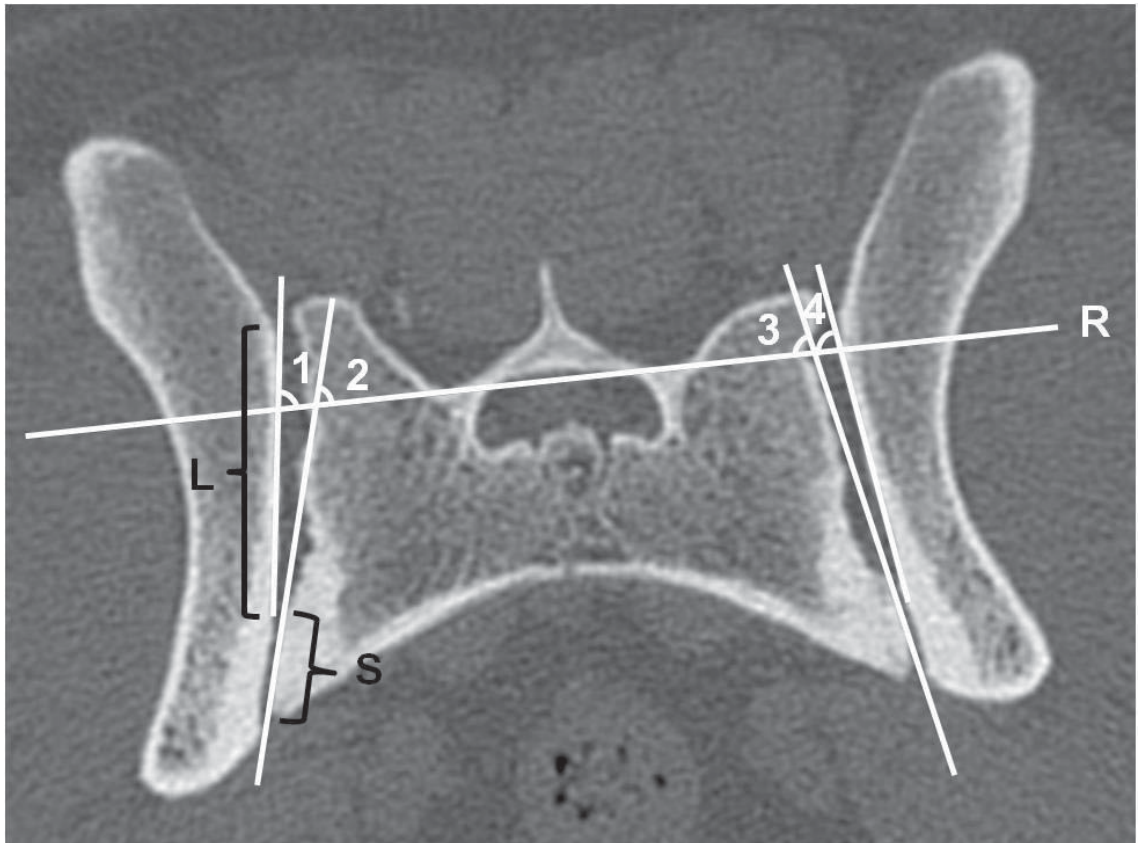


**Figure 2-1 Measurements of the inclination angles of the synovial components (S) and the ligamentous components (L) of the sacroiliac joint at the caudal location measured from the reference line (R). 1) The inclination angle of the right caudal ligamentous component; 2) the inclination angle of the right caudal synovial component; 3) the inclination angle of the left caudal synovial component; 4) the inclination angle of the left caudal ligamentous component**

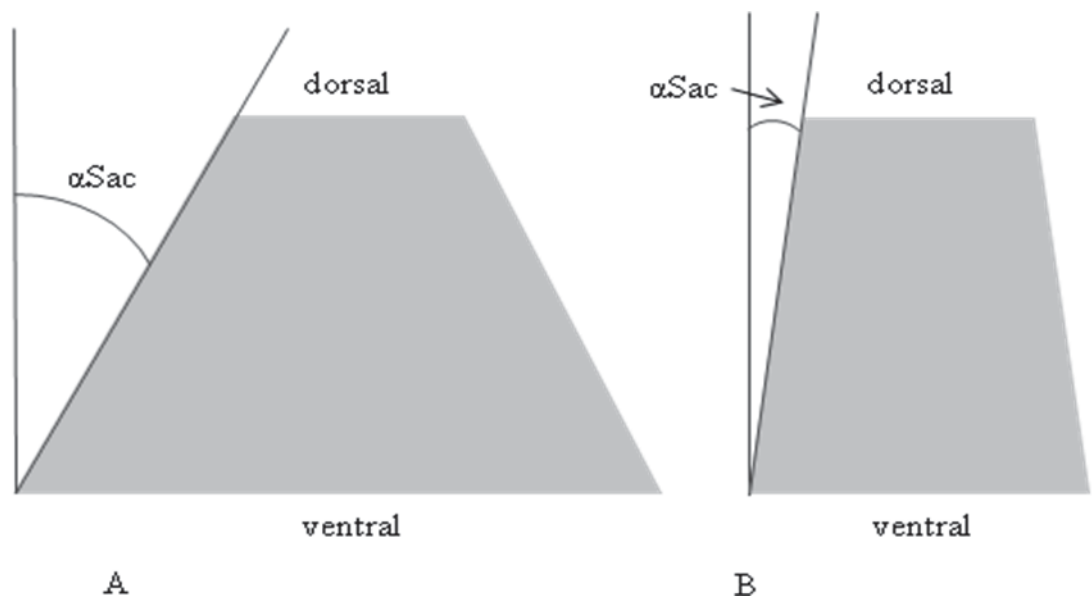


**Figure 2-2 A schematic representation of the inclination angles of the sacrum: A) representation of a more oblique inclination angle B) representation of a more sagittal inclination angle**

## **2.2. Materials and methods**

### *2.2.1.1. Breed selection*

German Shepherd dogs were selected for use in these studies because they are acknowledged to have a breed predilection for diseases causing lumbosacral region pain (Schulman and Lippincott, 1988). German Shepherd dogs are commonly used as military and police dogs (Moore et al., 2001; Evans et al., 2007). These dogs are socially and economically valuable animals, and lumbosacral region pain can be career limiting. It may be that the intense, repetitive motions performed by working dogs may have an impact on overloading the SIJ (Gembardt, 1974), but the involvement of the SIJ in lumbosacral region pain is unknown.

Greyhounds (GHs) were selected as a breed for comparison to GSDs because they are of comparative size, athletic ability and have a low incidence of lumbosacral region pain at the Massey University Veterinary Teaching Hospital.

### *2.2.2. Dogs*

The use of dogs in this study was approved by the Massey University Animal Ethics Committee. The study group consisted of dogs (GSDs and GHs) which were not currently affected by lumbosacral region pain. There were 10 GSDs from the New Zealand Police Department that had no history of pelvic limb lameness or reduced performance (for example, decreased ability or willingness to jump, or reduced enthusiasm for attack training), and that were in training or actively in service. These dogs either presented to the Massey University Veterinary Teaching Hospital for a clinical problem unrelated to lumbosacral region pain or pelvic limb pain, or were healthy dogs that were recruited directly for the study from healthy police dogs whose handlers agreed to allow a lumbosacral CT scan to be performed on the dog. Twelve racing GHs were recruited from a local trainer. Permission was obtained for the dogs to undergo CT scans of the lumbosacral region. These dogs were currently racing, and had no history of pelvic limb lameness or reduced performance.

All study participants underwent visual gait assessment, a pelvic limb orthopaedic examination, and a spinal neurological examination by a specialist surgeon to exclude potential causes of pelvic limb lameness. The pelvic limb orthopaedic examination

included abduction and extension of the coxofemoral joints. To detect lumbosacral region pain, pressure was applied over the lumbosacral joint, and the joint was extended with a fulcrum placed at the lumbosacral junction (lumbosacral lordosis test) (Worth et al., 2009). The neurological examination included an assessment of gait, conscious proprioceptive responses, myotactic reflexes, anal tone and perineal sensation. Additionally, the pelvic limb toenails were examined for evidence of scuffing indicating neurological abnormalities or musculoskeletal weakness. Dogs were excluded if there was evidence of pain or neurological abnormalities. Following CT scan acquisition, dogs were excluded from the study if either transitional vertebrae or degeneration of the lumbosacral intervertebral disc were evident.

### 2.2.3. CT scan procedure

A Philips Brilliance 16 slice multi-detector helical CT scanner<sup>1</sup> was used to perform the scans. The scans were constructed in bone and soft tissue algorithms with 1 mm thick slices overlapping by 0.5 mm. The scans were performed under anaesthesia, using either a combination of intravenous medetomidine<sup>2</sup> (0.005-0.01 mg/kg) and butorphanol<sup>3</sup> (0.2-0.3 mg/kg), or intravenous propofol<sup>4</sup> to effect, followed by inhalation maintenance using isoflurane.<sup>5</sup>

Positioning for the CT scans was standardised for all dogs. Positioning was designed to achieve the full extent of passive physiologic range of motion in flexion and extension (Demoulin et al., 2007). The dogs were placed in dorsal recumbency with a padded trough underneath the lumbar spine and pelvis. The flexed position involved drawing the pelvic limbs forward beside the chest with weights, until the caudal pelvis was just elevated off the table (Figure 2-3). This positioning produced full flexion of the lumbosacral, sacroiliac and coxofemoral joints. The extended position was achieved by extending the pelvic limbs caudally until the femurs were nearly parallel to the lumbar spine. Pressure was manually applied in a caudoventral direction to the proximal pelvic

---

<sup>1</sup> Philips Healthcare, Eindhoven, The Netherlands

<sup>2</sup> Pfizer Animal Health, New South Wales, Australia

<sup>3</sup> Ilium Drugs registered to Troy Laboratories Pty Ltd, New South Wales, Australia

<sup>4</sup> Norbrook NZ Ltd, Auckland, New Zealand

<sup>5</sup> Piramal Healthcare Ltd, India



limbs until the cranial aspect of the pelvis began to lift from the table. This completely strained all motion segments of the caudal spine to reach the end of their physiologic range of motion. The limbs were positioned so that each patella was centrally aligned over the dorsal, distal femur, so that there was no abduction or adduction of the limb (Figure 2-4, Figure 2-5). Neutral position involved positioning the femurs perpendicular to the lumbar spine, pelvis and couch, with the dog still in dorsal recumbency, by flexing the coxofemoral joints and generating flexion at the lumbosacral and sacroiliac joints. The positioning of the dogs was aimed to represent the full extent of passive range of motion of the sacroiliac, lumbosacral and coxofemoral joints by positioning them in the limits of flexion and extension. Realising that range of motion varies between dogs; the dogs were positioned to achieve full passive extension and flexion in a way that the end of physiologic motion was reached for each individual dog. This was assessed by the use of the subjective assessments stated above.

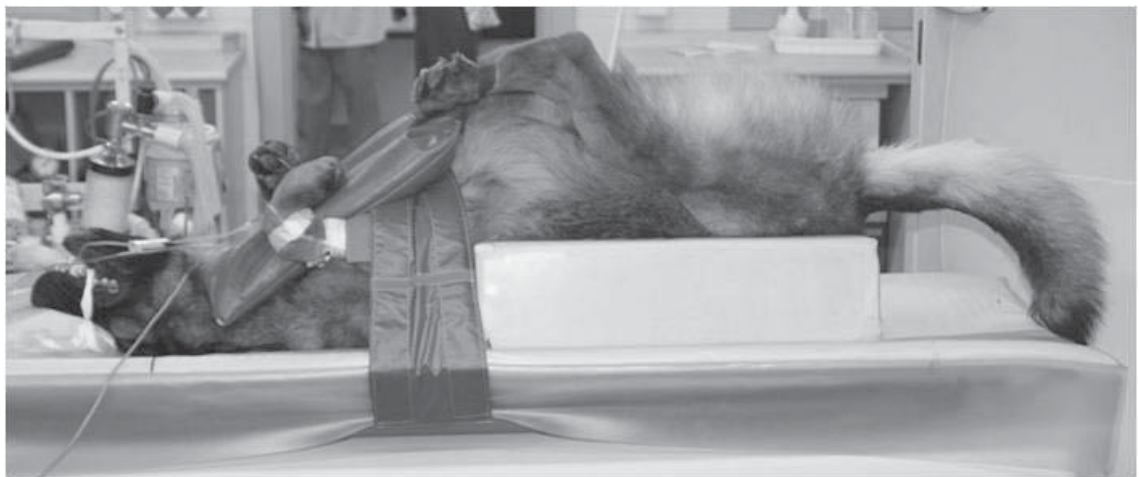


**Figure 2-3 Computed tomography positioning for the flexed position; lateral view**



**Figure 2-4 Computed tomography positioning for the extended position; lateral view**



**Figure 2-5 Computed tomography positioning for the extended position; caudal view**

#### 2.2.4. Motion

##### *2.2.4.1. Motion methodology development*

The aim of this technique was to describe motion at the SIJ. Rotational and translational motions have been previously measured in the human SIJ, and therefore these components were assessed. Initially, motion of the SIJ was defined as the movement of the joint surface on the sacrum relative to the ilium. It was hoped that by doing this, a centre of rotation would be able to be determined and motion of the synovial component and the ligamentous component isolated. A limitation of this method was the shape of the joint surface. The shape of the surface of the entire joint, and the shape of the synovial joint component varied between dogs. This made it hard to find consistent landmarks that could be used to measure motion on all the dogs. Additionally, the complete borders of the joint surface were difficult to definitively identify on volume rendered CT scans (Figure 1-1). This meant that the exact location of the extent of the joint surface could not reliably be identified between flexion and extension. These limitations lead to the decision to measure motion of the ilium relative to the sacrum with the assumption that this represented motion of the SIJ.

The second method attempted was placing lines on sagittal slice images of the sacrum and ilium. This method involved displaying a targeted volume rendered image with the axial margin representing the middle of the vertebral canal in the sagittal plane (Figure 2-6). A line was placed along the ventral surface of the dorsal sacral lamina (Figure 2-6). The volume rendered image was then expanded to include the ilium, and a line was placed on the ilium (Figure 2-7). Motion was to be compared between the ilial line and the sacral line. A major limitation of this method was identified that prevented its use: some of the dogs were slightly rotated in the sagittal plane during scanning. Due to limitations of the software, this obliquity could not be corrected to allow a parasagittal volume reconstruction in the true dorsoventral plane. Therefore, the lines placed on the images in flexion and extension would not have been located in the exact same position.

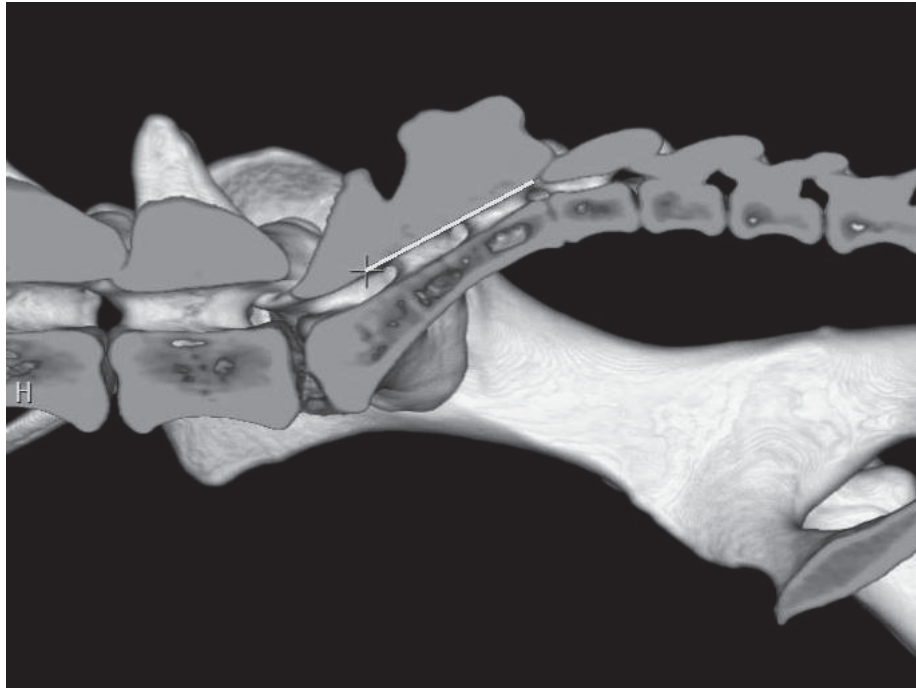


**Figure 2-6** A volume rendered image was targeted until the midline of the sacrum was displayed. A line was placed along the ventral surface of the dorsal sacral lamina.

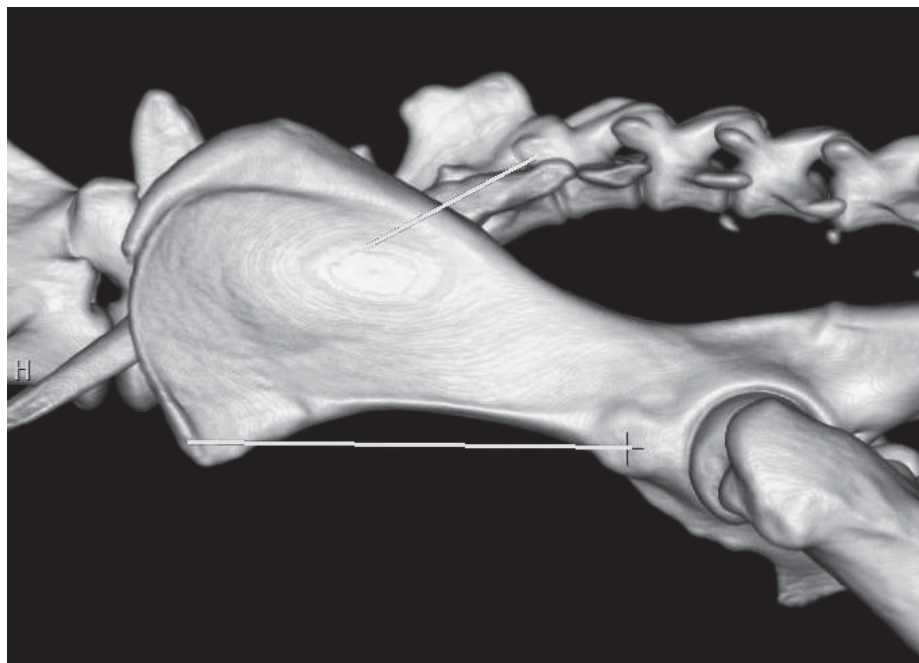


**Figure 2-7** The rendered image was expanded until the ilium was again visualised overlying the sacrum, and a line was placed on the ilium.

Finally, it was decided to measure motion of the ilium relative to the sacrum from reference lines placed between bony landmarks on the ilial surface and the sacral surface.

In order to quantify motion of the ilium relative to the sacrum, calculations were performed to determine translational motion (which was comprised of components in the X- and Y- axes) and rotational motion of the ilium relative to the sacrum around an unknown pivot point. The X-axis was set as the sacral line along the dorsal spinous processes of the sacrum. The Y-axis was set at ninety degrees to the X-axis.

#### *2.2.4.2. Measurement performance*

Lines were placed on volume rendered images of the ilium and the sacrum using anatomical points that could be accurately and precisely identified on both the flexed and extended scans (Figure 2-8). The sacral lines were placed between points on the dorsal spinous processes of the sacrum. The ilial lines were typically placed between points on the tuber coxae and the body of the ilium. The lines were placed so that if they were to be extended they would intersect at an acute angle. The exact anatomical points used to place the lines varied between dogs, and between left and right ilia, due to normal anatomical variations, and limitations of the scan length, but were identical between the flexed and extended scans of any particular dog. As it was the motion (rotation and translation) of the ilium relative to the sacrum that was compared between dogs, the exact placement of the sacral and ilial lines was only important between the flexed and extended views of the same dog. A line described by any two points on a bone would move in the same way as any other line fixed on that bone. Therefore, any two points could be used to place the lines, and these points did not need to be the same between dogs. This allowed the selection of the most prominent points for each dog. The volume rendered study on which the lines were placed, were constructed on a Philips Extended Brilliance Workstation.<sup>6</sup>

After manipulating the volume rendered study to symmetrically align the ilia, a display image depicting the ilial and sacral lines without the bones present was saved (Figure 2-9). Line placement and subsequent saving of the corresponding display image was

---

<sup>6</sup> Brilliance Workstation version 4.5.2.40007, Philips Healthcare, Eindhoven, The Netherlands

performed three times for each position. The left and right limbs were measured and analysed independently to allow comparisons to be made between sides.

The images of the lines were calibrated and measured on ClearCanvas Workstation.<sup>7</sup> An angle marker was drawn to overlies the ilial and sacral lines (Figure 2-10). This marker was used to locate the intersection point of the lines, and to measure the angular difference between the lines. The distances from the intersection point to the cranial and caudal points of the ilial and sacral lines were measured in flexion and extension. The cranial points of the ilial and sacral lines were denoted by subscript number 1 and the caudal points of the lines were denoted by subscript number 2.

---

<sup>7</sup> ClearCanvas RIS/PACS Freeware Version 2.0.12729.37986 SP1. ClearCanvas Inc, Toronto, Canada.

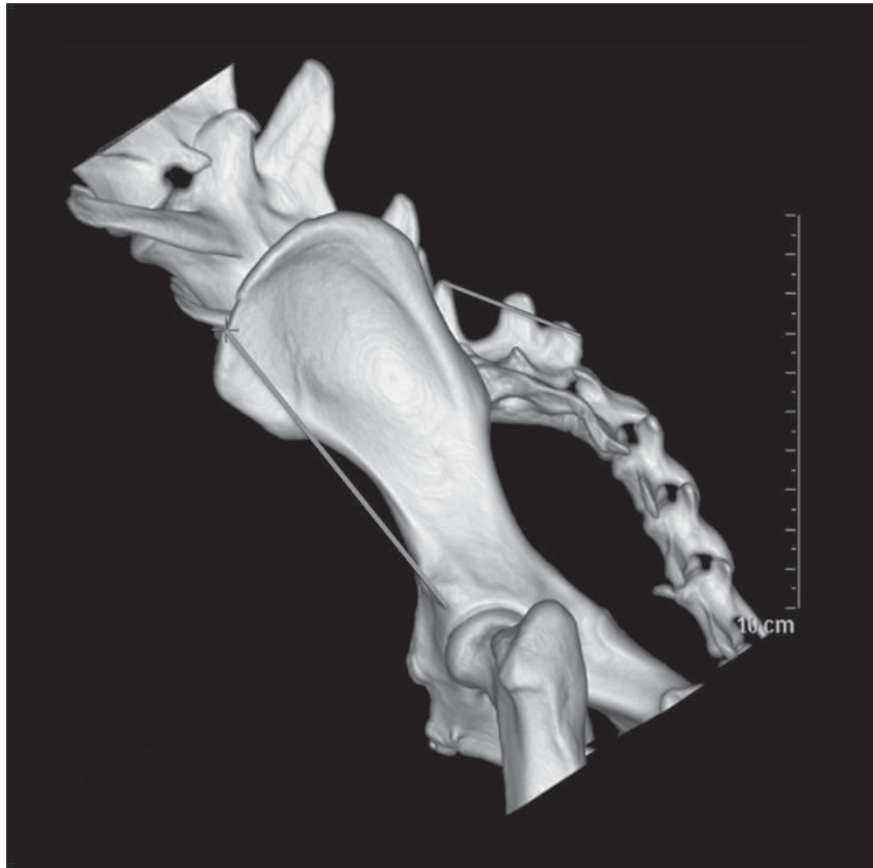


**Figure 2-8 Placement of the ilial and sacral lines on the volume rendered computed tomography images of the ilium and sacrum**

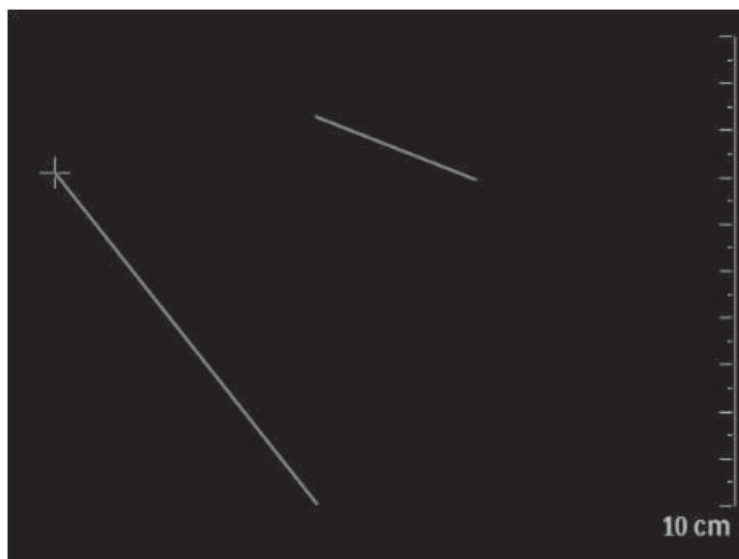


**Figure 2-9 Display image of the ilial and sacral lines upon which measurements were performed**



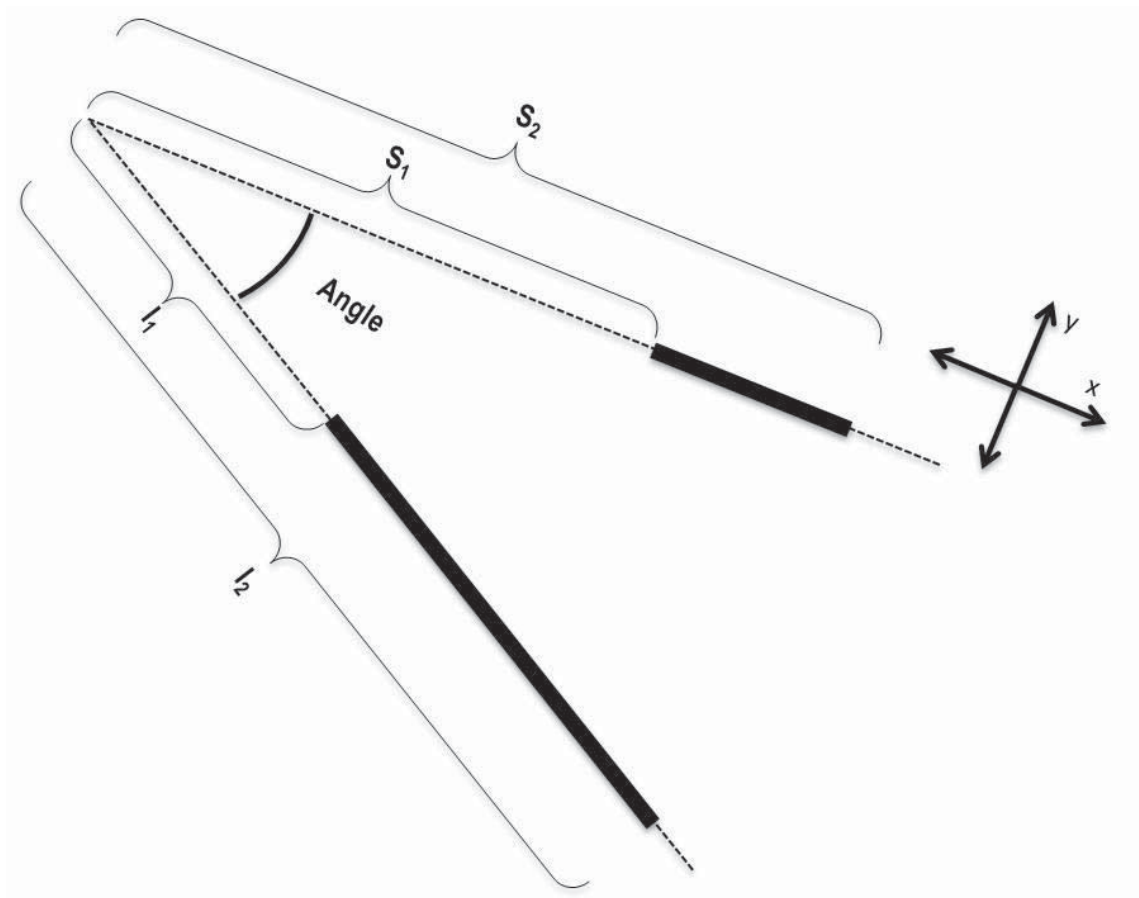


**Figure 2-10 Measurements performed on the ilial and sacral lines using ClearCanvas Workstation. An angle marker (dotted line) was placed over the ilial and sacral lines (solid black lines) to determine the angle (degrees) of their intersection point. Measurements were made of the distances (cm) from the intersection point to the cranial point of the sacral line ( $S_1$ ), the caudal point of the sacral line ( $S_2$ ), the cranial point of the ilial line ( $I_1$ ), and the caudal point of the ilial line ( $I_2$ ). The sacral line was set as the X-axis, with the Y-axis set perpendicular to the X-axis**

#### *2.2.4.3. Range of motion calculations*

The lengths of the ilial (I) and sacral (S) lines were calculated in flexion and extension to confirm point placement. The ilial line was defined as ( $I_{2F}-I_{1F}$ ) in flexion, and ( $I_{2E}-I_{1E}$ ) in extension. The sacral line was defined as ( $S_{2F}-S_{1F}$ ) in flexion, and ( $S_{2E}-S_{1E}$ ) in extension. All further calculations were performed on the averages of the triplicate



measurements ( $I_{1F}$ ,  $I_{2F}$ ,  $S_{1F}$  and  $S_{2F}$ ,  $I_{1E}$ ,  $I_{2E}$ ,  $S_{1E}$  and  $S_{2E}$ , and  $\phi_F$  and  $\phi_E$ ). Measurements could be made to a precision of  $0.1^\circ$  and 0.01 cm on ClearCanvas Workstation.

The images of the lines in flexion and extension were placed so that the flexed and extended  $S_1$  points were superimposed, with the sacral lines positioned on the X-axis (Figure 2-11). The positions of the  $S_2$  points were then superimposed, confirming that the length of the ilial lines was the same between flexion and extension. This produced a shift ( $ds$ ) in the position of the extended intersection point ( $E_0$ ) along the X-axis calculated by  $S_{1F} - S_{1E}$ . This allowed coordinate calculations to be performed relative to an origin placed at the flexed intersection point ( $F_0 = 0,0$ ). The flexed position was used as the reference position from which to measure motion between flexion and extension. A triangle was formed between the flexed and extended ilial lines, for which the values of one angle ( $\phi_E$ ) and one side ( $ds$ ) were known. The value of the supplementary angle ( $\phi_F$ ) was also known, allowing the remaining two angles within the triangle to be calculated according to Equations 1 and 2.

$$(180 - \phi_F) \quad \text{Equation 1}$$

$$(\phi_F - \phi_E) \quad \text{Equation 2}$$

The distance ( $d$ ) from  $E_0$ , to the pivot point of the ilial lines ( $X_p, Y_p$ ) was calculated according to Equations 3, 4, 5, and 6.

$$\frac{a}{\sin A} = \frac{b}{\sin B} \quad \text{Equation 3}$$

$$\frac{d}{\sin(180 - \phi_F)} = \frac{ds}{\sin(\phi_F - \phi_E)} \quad \text{Equation 4}$$

$$d \sin(\phi_F - \phi_E) = ds \sin(180 - \phi_F) \quad \text{Equation 5}$$

$$d = \frac{ds \sin(180 - \phi_F)}{\sin(\phi_F - \phi_E)} \quad \text{Equation 6}$$

The X and Y coordinates of the pivot point ( $X_p, Y_p$ ) were calculated relative to the origin according to Equations 7 and 8.

$$X_p = d \cos \phi_E - ds \quad \text{Equation 7}$$

$$Y_p = d \sin \phi_E \quad \text{Equation 8}$$

The distance (r) along the flexed ilial line from (X<sub>p</sub>,Y<sub>p</sub>), to the cranial point of the flexed ilial line (X<sub>IIF</sub>,Y<sub>IIF</sub>) was calculated according to Equations 9 -14 (Figure 2-12), where dx<sub>r</sub> and dy<sub>r</sub> are defined by Equations 11 and 12. The value r is the radius of rotation of X<sub>IIF</sub>,Y<sub>IIF</sub> around X<sub>p</sub>,Y<sub>p</sub>.

$$r^2 = a^2 + b^2 \quad \text{Equation 9}$$

$$r^2 = dx_r^2 + dy_r^2 \quad \text{Equation 10}$$

$$dx_r = X_p - X_{IIF} \quad \text{Equation 11}$$

$$dy_r = Y_p - Y_{IIF} \quad \text{Equation 12}$$

$$r = \sqrt{dx_r^2 + dy_r^2} \quad \text{Equation 13}$$

$$r = \sqrt{(X_p - X_{IIF})^2 + (Y_p - Y_{IIF})^2} \quad \text{Equation 14}$$

The flexed ilial line was rotated around X<sub>p</sub>,Y<sub>p</sub> until it overlaid the extended ilial line. This provided the location upon the extended ilial line where the cranial point of the flexed ilial line (X<sub>1</sub>',Y<sub>1</sub>') was predicted to move to if all motion was due to rotation. Coordinates of X<sub>1</sub>',Y<sub>1</sub>' were calculated relative to X<sub>p</sub>,Y<sub>p</sub> by Equations 15 and 16. These calculations were repeated for the predicted position of the caudal end of the extended ilial line (X<sub>2</sub>',Y<sub>2</sub>') using X<sub>I2F</sub> and Y<sub>I2F</sub>.

$$X_1' = c \cdot \cos \phi_E \quad \text{Equation 15}$$

$$Y_1' = c \cdot \sin \phi_E \quad \text{Equation 16}$$

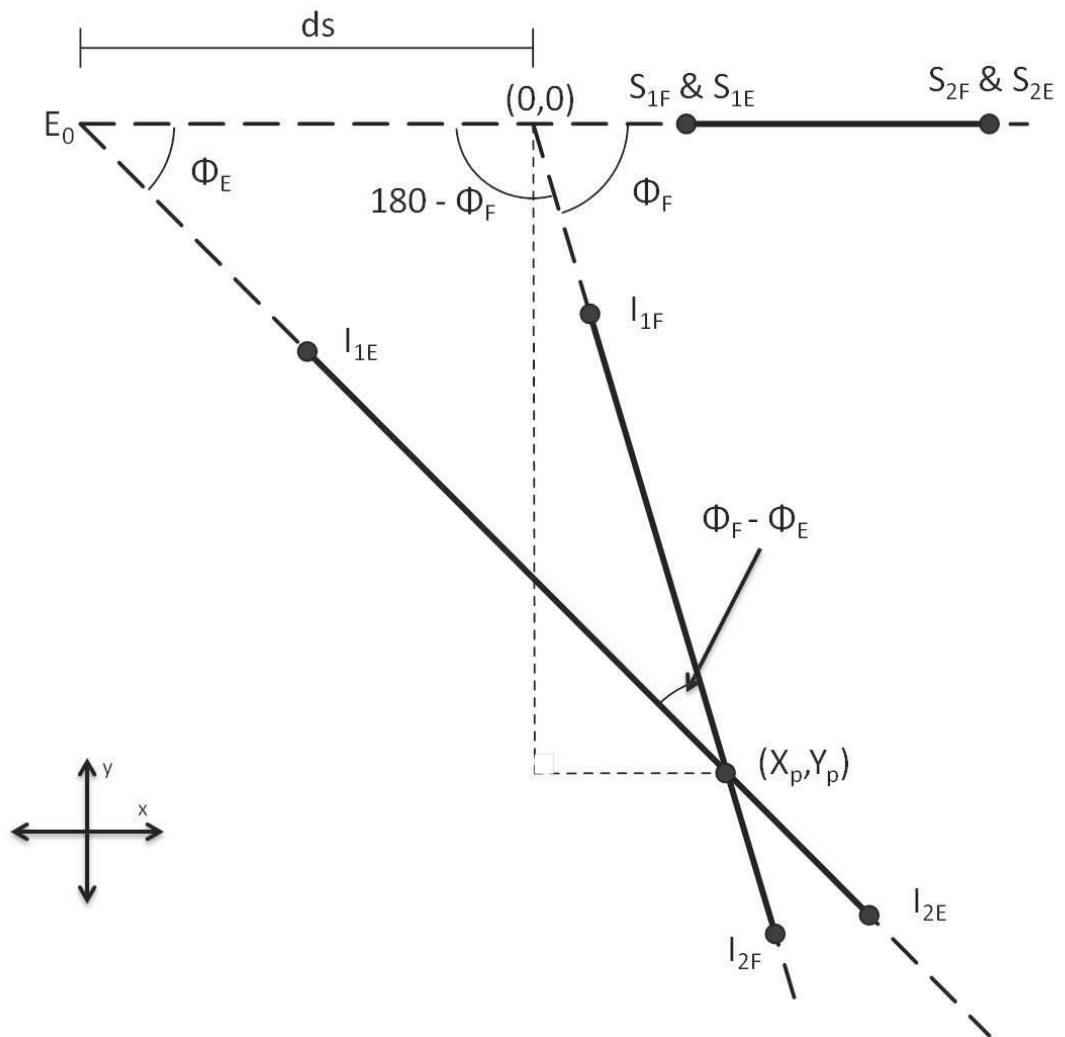


**Figure 2-11 Schematic diagram of the calculations performed to determine the coordinates of the pivot point of the flexed and extended ilial lines  $(X_p, Y_p)$  relative to the origin  $(0,0)$**

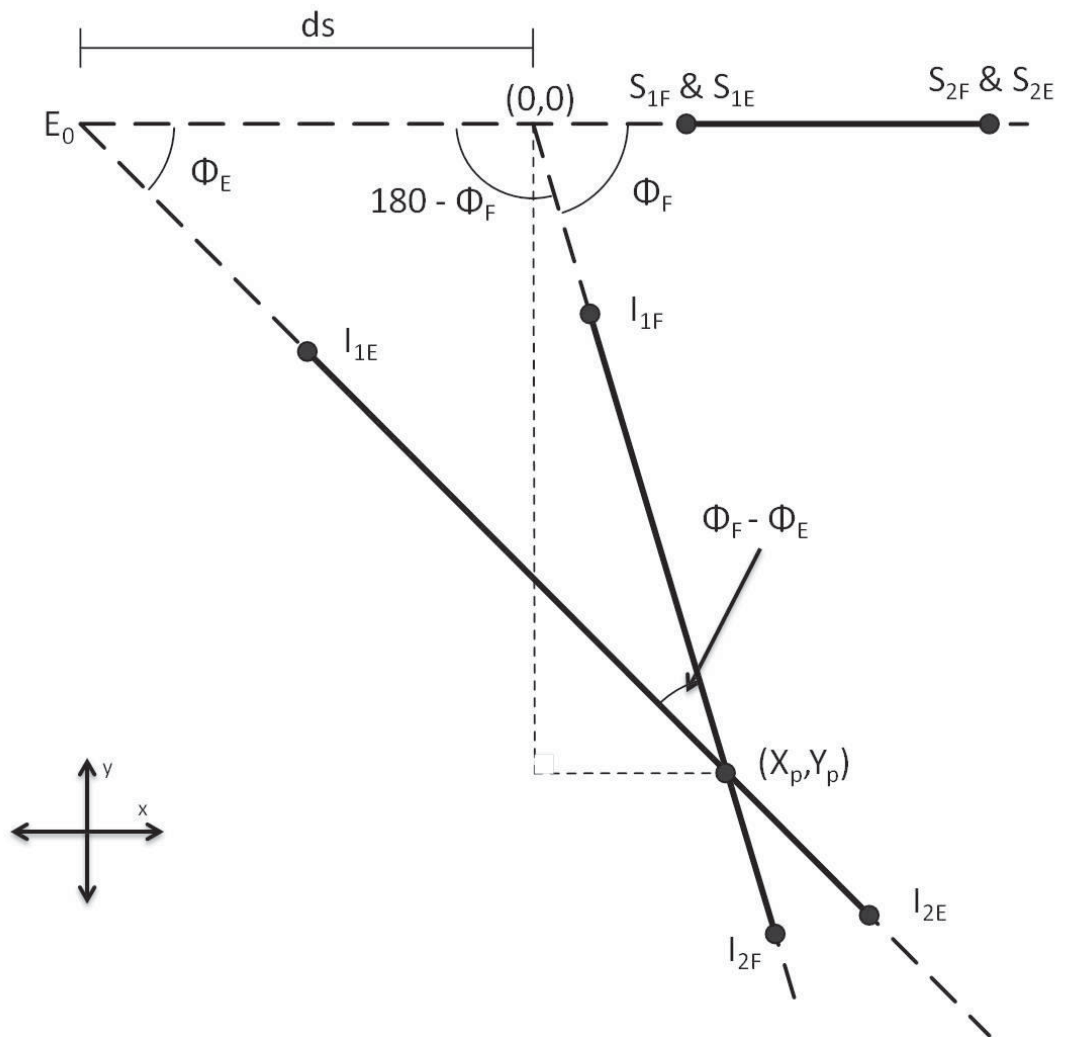


**Figure 2-12 Schematic diagram of the calculations performed to determine the X-axis and Y-axis translational movement of the ilial line between flexion and extension**

The difference between the measured location of the cranial point of the extended ilial line ( $X_{IIE}, Y_{IIE}$ ), and the predicted location of the cranial point of the ilial line due to rotation ( $X_1^{\circ}, Y_1^{\circ}$ ), was assumed to be the net translational motion (made up of X-axis and Y-axis components). A graph was plotted to help determine the location of  $X_1^{\circ}, Y_1^{\circ}$ . The coordinates of  $X_1^{\circ}, Y_1^{\circ}$  were converted to be relative to the original origin by Equation 17 (depending on the location of  $X_1^{\circ}, Y_1^{\circ}$  with respect to the pivot) (Figure 2-13).

$$[(X_p \pm X_1^{\circ}), (Y_p \pm Y_1^{\circ})] \quad \text{Equation 17}$$

The X-axis component of translational motion of the cranial point of the ilial line between flexion and extension ( $dx_1$ ) was calculated by the difference between these two points, according to Equation 18. The Y-axis component of translational motion ( $dy_1$ ) was calculated according to Equation 19.

$$dx_1 = X_{IIE} - X_1^{\circ} \quad \text{Equation 18}$$

$$dy_1 = Y_{IIE} - Y_1^{\circ} \quad \text{Equation 19}$$

These calculations were repeated to find  $dx_2$  and  $dy_2$  for the caudal point of the ilial line using  $I_{2E}$  and  $X_2^{\circ}$ . The average translational motion of the ilium relative to the sacrum ( $dx$  and  $dy$ ) was calculated by averaging  $dx_1$  and  $dx_2$ , and  $dy_1$  and  $dy_2$ . All calculations were performed on left and right SIJs separately.

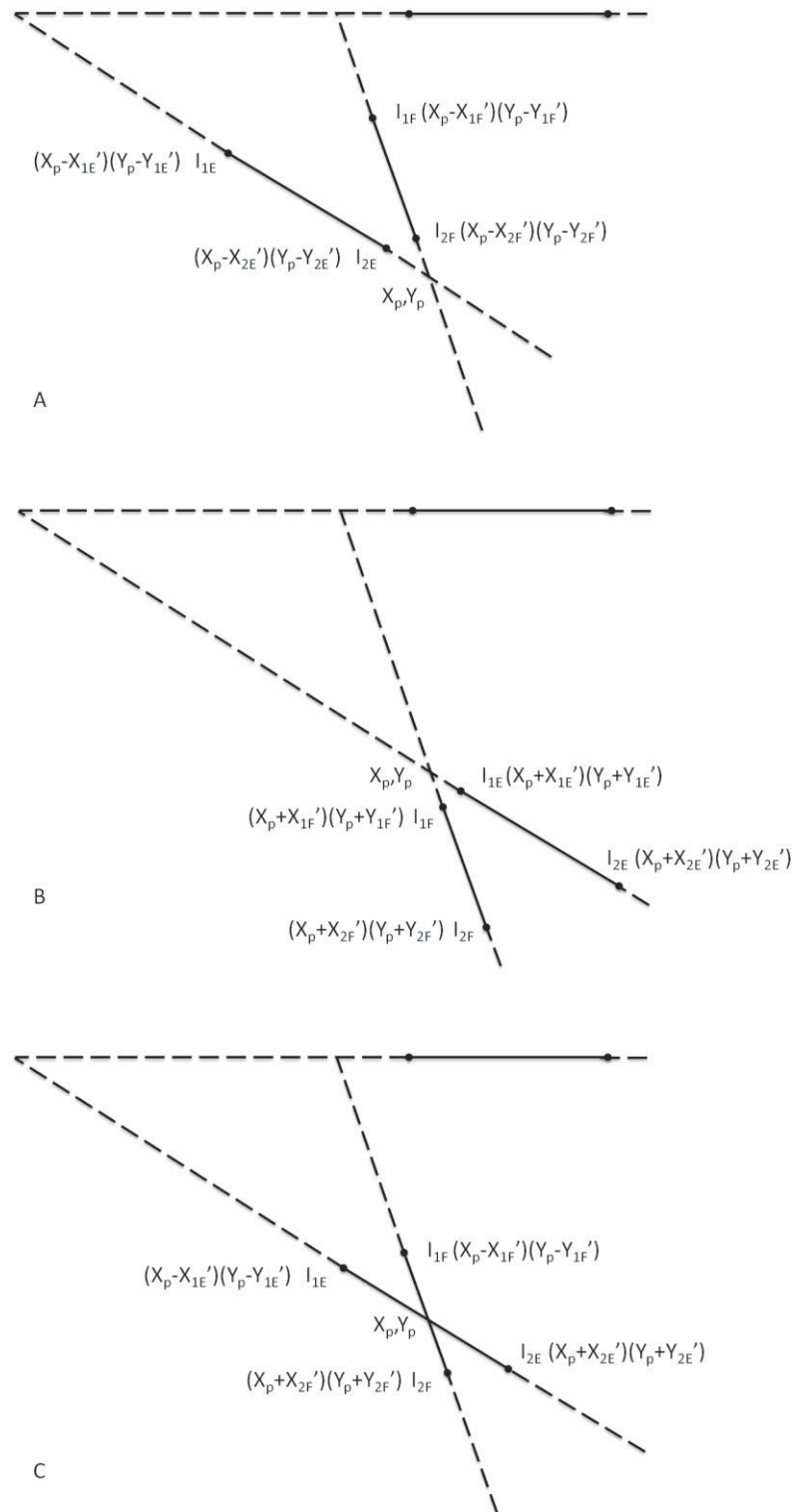


**Figure 2-13 Schematic diagram to determine calculations to convert  $X_1', Y_1'$  relative to the origin, for situations where the ilial and sacral lines fall between the origin and  $X_p, Y_p$  (A), where the ilial and sacral lines both fall on the far side of  $X_p, Y_p$  (B), and where the cranial and caudal points fall on either side of  $X_p, Y_p$  (C)**

#### 2.2.4.4. Definitions

$F_0$  = The intersection point of the ilial and sacral lines in flexion

$E_0$  = The intersection point of the ilial and sacral lines in extension

$\phi$  = The average of the triplicate measured values (in degrees) of the angle formed by the intersection of the ilial and sacral lines, in the flexed position  $\phi_F$  and in the extended position  $\phi_E$

$I_1$  = The average of the triplicate measured distance (cm) from the intersection point of the ilial and sacral lines, to the cranial end of the ilial line, in the flexed position ( $I_{1F}$ ) and the extended position ( $I_{1E}$ )

$I_2$  = The average of the triplicate measured distance (cm) from the intersection point of the ilial and sacral lines, to the caudal end of the ilial line, in the flexed position ( $I_{2F}$ ) and the extended position ( $I_{2E}$ )

$S_1$  = The average of the triplicate measured distance (cm) from the intersection point of the ilial and sacral lines, to the cranial end of the sacral line, in the flexed position ( $S_{1F}$ ) and the extended position ( $S_{1E}$ )

$S_2$  = The average of the triplicate measured distance (cm) from the intersection point of the ilial and sacral lines, to the caudal end of the sacral line, in the flexed position ( $S_{2F}$ ) and the extended position ( $S_{2E}$ )

$X_p, Y_p$  = The coordinates of the pivot point of the flexed and extended ilial lines

$X', Y'$  = The predicted location of the cranial ( $X_1', Y_1'$ ) and caudal ( $X_2', Y_2'$ ) points of the ilial line, if motion was due to rotation only

$X_{IE}, Y_{IE}$  = The coordinates of the cranial ( $X_{IIE}, Y_{IIE}$ ) and caudal ( $X_{I2E}, Y_{I2E}$ ) points of the ilial line in extension

$X_{IF}, Y_{IF}$  = The coordinates of the cranial ( $X_{IIF}, Y_{IIF}$ ) and caudal ( $X_{I2F}, Y_{I2F}$ ) points of the ilial line in flexion

$d\phi$  = The rotational motion of the ilium relative to the sacrum, between flexion and extension, calculated from the differences of the averages of the measured angles in flexion ( $\phi_F$ ) and extension ( $\phi_E$ )

$dx$  = The translational motion in the X-axis of the ilium relative to the sacrum, between flexion and extension (cm)

$dy$  = The translational motion in the Y-axis of the ilium relative to the sacrum, between flexion and extension (cm)

### 2.2.5. Inclination angles

#### 2.2.5.1. *Inclination angle methodology development*

Inclination angle measurements were performed on transverse slice images of the neutral position scan in a bone algorithm. These slices were aligned to the cranial endplate of the first sacral vertebra so that the images sliced through the sacrum and SIJ in a consistent plane. The irregular shape of the SIJ meant that distribution of the ligamentous and synovial joint components was different between the cranial and the caudal joint surface (Figure 1-1). For this reason, inclination angles were measured at both a cranial and a caudal location. Cranial inclination angle measurements were initially performed where the dorsal sacral laminae fused. German Shepherd dogs had cranial overhang of the dorsal sacral laminae, causing the cranial position to be located more cranially than in GHs, and in a position that did not transect the synovial component of the joint. Therefore, the most cranial extent of the synovial component of the joint was used as the location of the cranial measurements in order to transect both the synovial component and the ligamentous component.

Initially, a line was placed down the SIJ space, and another line placed along the ventral surface of the sacrum, along a tangent to the left and right ventrolateral sacral edges (Figure 2-14). The inclination angle was measured at the intersection of these two lines. Development of degenerative osteophyte spurs on the ventral margins of the sacrum produced variability in the location of the ventral marker between dogs, and between cranial and caudal locations within the same dog (Figure 2-14). The location of a line along the dorsal surfaces of the wings of the sacrum also varied in location due to



osteophyte production (Figure 2-15). Finally, a line was placed across the left and right dorsal sacral laminae at their lowest points (Figure 2-16). This line was used as a reference line.

A line placed to bisect both the ligamentous and synovial components of the joint, invariably did not represent the inclination angle of either component. For this reason, the inclination angles of the ligamentous and synovial components of the joint were measured individually.

The decision of where to place a line that bisected the joint space was subjective, and there was a degree of variability in the “best” position for the line (Figure 2-17). Additionally, the joint space in many dogs was not a linear entity, but had ridges of bone displacing the joint space, as described by authors of previous studies (Gregory et al., 1986). This meant that variability was introduced into the method by the inability to repeatedly place a line down the joint space. Alternatively, it was noted that the medial surface of the ilium was found to have a repeatedly flat surface along which a line could be passed. The lateral surface of the sacrum was identified to be the most consistently flat surface of the synovial component upon which to place a line. Thus, it was decided to use the medial surface of the ilium to represent the inclination angle of the ligamentous component, and the lateral surface of the sacrum to represent the inclination angle of the synovial component.

The final method for measuring the inclination angles of the SIJ involved placing a line down the medial surface of the ilium along the ligamentous component, and a line along the lateral surface of the sacrum in the synovial component, and measuring the inclination angle off a reference line placed along the lowest points in the dorsal sacral laminae (Figure 2-1).



**Figure 2-14** Lines were placed along the sacroiliac joint space, and along the ventral surface of the sacrum, along a tangent to the left and right ventrolateral sacral edges. The location of osteophyte on the ventral sacrum in some dogs (arrow) which produced variability in marker location.



**Figure 2-15** Lines were placed along the sacroiliac joint space, and along the dorsal surfaces of the wings of the sacrum.



**Figure 2-16** The lowest points in the dorsal sacral laminae (arrows) were used to position a reference line.





**Figure 2-17 Transverse section through the sacroiliac joints with two inclination angle markers on the right sacroiliac joint showing potential variation in placement of marker along the axis of the joint space.**

#### 2.2.6. Measurement performance

The neutral position scan was used to measure inclination angles in the absence of excessive strain from full extension or flexion. The original CT scans were manipulated on a Philips Extended Brilliance Workstation to align the scan to the cranial endplate of the first sacral vertebral segment, and to produce a bilaterally symmetrical image, in order to standardise measurements. Measurements of the inclination angles were performed using eFilm Workstation<sup>8</sup> instead of ClearCanvas because one reference line could be used to measure the inclination angles of all four joint components, with fewer steps than what would be necessary in ClearCanvas. The inclination angles of the

---

<sup>8</sup> eFilm version 2.1, Merge Healthcare, Chicago, Illinois

synovial and ligamentous components of the left and right SIJs were measured at a cranial and caudal location.

The synovial component of the joint was identified by narrowing of the joint space ventrally, the presence of thick subchondral bone and a lack of fibrous and adipose tissue present within the joint space. The dorsally positioned ligamentous component was identified by a wider joint space and the presence of short soft tissue fascicles interposed with adipose tissue within the joint space. The cranial location for measurements was identified by scrolling caudally through the sacrum to the first point where the ventral synovial component of the joint was visible, as depicted by narrowing of the joint space, and the presence of increased subchondral bone density. The caudal location was identified by the position of ventral deviation of the dorsal foramina of the second sacral segment from the vertebral canal. A reference line was placed along the lowest points in the dorsal sacral laminae. The inclination angles of the SIJ were approximated by measuring the inclination angle of the ilial or sacral bone face at the margin of the joint space. These structures were used to increase repeatability of the measurements by providing a flat surface upon which to measure, and by removing the error associated with measuring the axis of a joint space of variable width. The medial surface of the ilium was selected for measurement of the inclination angle of the ligamentous component because it was a consistently flat surface. Likewise, the flattest surface for measurement of the synovial component was the lateral surface of the sacrum. The inclination angle was defined as the angle between the axis of the joint space and the reference line in the dorsal plane (Figure 2-1). Larger inclination angles indicate that the joint axis is orientated closer to the sagittal plane. These measurements were performed in triplicate. eFilm measurements could be performed to a precision of 1°.

#### 2.2.7. Statistical analysis

Data were analysed using the statistical software, R.<sup>9</sup> A mixed linear model that included a random intercepts term for each dog was used to analyse the effects of age, bodyweight, limb, sex and breed on the measurements of rotational motion ( $\phi$ ), translational motions in the X- and Y- axes, the inclination angles, and their

---

<sup>9</sup> R version 15.1, R Foundation for Statistical Computing, Vienna, Austria

interactions. The mixed model adjusted for repeated measures on each dog due to left and right limbs, and was fitted using the restricted maximum likelihood (REML) procedure in R. Differences were considered significant at  $p < 0.05$ . All data were collected in triplicate and results were averaged. All measurements were performed by the same observer with the observer blinded to results from previous trials. Intra-observer variability was determined from the coefficient of variance calculated from 6 measurements of each parameter, measured in both flexion and extension on one dog. All data were tested for normality using the Anderson-Darling test. Outliers from the fitted linear model were identified by examining the plot of standardised residuals against leverage. Identification of outliers was performed using analysis of Cook's distance. Cook's distance assesses the influence of a data point on the set of regression coefficients in a model. Data points with high influence can have a disproportionate impact on the model, producing misleading results. An outlier is an example of an influential data point (Christensen, 2011). Dogs with a Cook's distance of  $>1$  were excluded for that variable. The power to detect a breed difference for each variable was tested using a power calculation for the general linear model and expressed as a probability. Unless otherwise stated, the data are presented as the mean of the three measurements,  $\pm$  standard deviation.

## **2.3. Results**

### **2.3.1. Study design**

One GSD and 2 GHs were removed from the study due to the presence of transitional vertebrae in the lumbosacral region. This produced a final study number of 9 GSDs and 10 GHs without lumbosacral region pain. The left SIJ of one GSD was excluded from the analysis of X- and Y- axis translation due to a high residual Cook's distance, resulting in normally distributed data. There were 4 female and 5 male GSDs. There were 5 female and 5 male GHs. The ages of the GSDs ranged from 1-6.5 years old, with an average age of 3.25 years. These dogs ranged in weight from 26-38 kg, with an average weight of 33.1kg. The GHs ranged in age from 2.4-5.9 years old with an average age of 3.63 years. Their weights ranged from 28-34.5 kg with an average of 31.2 kg.

### 2.3.2. Method validation

The methods presented for the CT measurement of SIJ motion and inclination angles were found to have low intra-observer variability, with the coefficients of variance for the measurements ranging from 0.17-1.29% for the motion measurements, and 0.55-2.45% for the inclination angle measurements.

### 2.3.3. Motion

Average motion values from the raw data are presented in Table 2-1. These values do not take into account the interaction between rotational motion and bodyweight. Model estimates for the variables which account for the interaction between bodyweight and rotational motion are presented in Table 2-2. A breed difference was found in rotational motion. German Shepherd dogs had significantly greater rotational motion than GHs ( $p=0.047$ ). Rotational motion decreased with increasing bodyweight in GSDs ( $p=0.067$ ), but not in GHs ( $p=0.797$ ). Although the bodyweight averages of the groups were not significantly different, the distribution of bodyweights of the dogs varied between groups (Figure 2-18). Left vs. right limb, sex and age had no significant effect on rotational motion.

The X-axis translation of GSDs was not significantly different than GHs ( $p=0.105$ ). The power to find a breed difference was 0.45. If there is a genuine difference of 0.4 mm between the breeds, and with the variance seen in this study, then to have an 80% chance of detecting the difference, a sample size of 50 dogs would be needed.

The average Y-axis translation was not significantly different between breeds ( $p=0.184$ ), however, our power to find a breed difference in the Y-axis translation was only 0.32. If there is a genuine difference of 1 mm between the breeds, and with the variance seen in this study, then to have an 80% chance of detecting the difference, a sample size of 253 dogs would be needed.



**Table 2-1 Raw data averages for the rotational and translational motion variables in German Shepherd dogs (GSD) and Greyhounds (GH). These averages do not take into account the interaction between rotational motion and bodyweight which is described by the model estimate equations in Table 2-2.**

Variable	Mean ( $\pm$ standard deviation) of the raw data	
	GSD	GH
Rotational motion	2.0 $\pm$ 1.5°	1.5 $\pm$ 0.7°
X-axis translational motion	1.0 $\pm$ 0.7 mm	1.4 $\pm$ 0.7 mm
Y-axis translational motion	0.6 $\pm$ 0.4 mm	0.7 $\pm$ 0.4 mm

#### 2.3.4. Inclination angles

A small difference between the breeds was found in the inclination angle of the cranial synovial component. The average inclination angle of the cranial synovial joint component was larger (i.e. more sagittal) in GSDs than GHs after taking into account the effect of age (1.5° for each year) ( $p=0.035$ ).

No significant difference was found between breeds in the inclination angle of the caudal synovial component ( $p=0.128$ ). There was no significant effect of age, weight, limb or sex on the inclination angle of the caudal synovial component. Our power to find a difference was 0.33. If there is a genuine difference of 5° between the breeds, and with the variance seen in this study, then to have an 80% chance of detecting the difference, a sample size of 52 dogs would be needed.

There was no statistical difference between breeds in the inclination angles of the cranial, and caudal ligamentous components ( $p=0.967$  and  $p=0.211$  respectively). Our power to find a breed difference was 0.33 for the caudal synovial component and 0.41 for the cranial ligamentous component. If there is a genuine difference in the inclination angle of the cranial ligamentous component of 4° between the breeds, then to have an 80% chance of detecting the difference, a sample size of 79 dogs would be needed. If there is a genuine difference of 5° between breeds in the inclination angles of the caudal synovial component, sample sizes that are impractically large would be required.

The ages of GSDs were clustered in two groups, with ages between 1-3 years old, and between 5.3-6.5 years old. No GSDs lay between these clusters. Conversely, the GH age distribution was clustered centrally between 2.4-5.9 years old.

**Table 2-2 Parameter estimates and their standard errors from a mixed-effects linear regression model of rotational motion and the inclination angle of the cranial synovial component of the sacroiliac joint in German Shepherd dogs (GSD) and Greyhounds (GH).**

Variable	Estimate	Standard Error	p value
<b>Rotational motion (°)</b>			
Intercept	2.25 <sup>*</sup>	3.53	0.531
BreedGSD	8.88 <sup>†</sup>	4.09	0.047
BreedGH:Weight	-0.02 <sup>‡</sup>	0.11	0.840
BreedGSD:Weight	-0.25 <sup>§</sup>	0.13	0.068
<b>Cranial synovial component (°)</b>			
Intercept	73.2 <sup>#</sup>	3.3	<2e-16
Age	1.5 <sup>**</sup>	0.8	0.087
BreedGSD	5.6 <sup>††</sup>	2.4	0.035

<sup>\*</sup> Intercept: For a Greyhound, the baseline level for rotational motion is 2.25° in the absence of the effect of weight

<sup>†</sup> BreedGSD: For a German Shepherd dog, the baseline level for rotational motion (°) is 11.13 (= 2.25 + 8.88) in the absence of the effect of weight

<sup>‡</sup> BreedGH:Weight: For a Greyhound, the rotational motion (°) = 2.25 – (bodyweight\*0.02)

<sup>§</sup> BreedGSD:Weight: For a German Shepherd dog, the rotational motion (°) = 11.13 – (bodyweight\*0.25)

# Intercept: For a Greyhound, the baseline inclination angle of the cranial synovial joint component is 73.2°

\*\* Age: The effect of age (1.5° for each year of age) is the same for both breeds

†† BreedGSD: For a German Shepherd dog, the inclination angle of the cranial synovial joint component (°) = (73.2 + 5.6) + 1.5 \* Age

## 2.4. Discussion

In this Chapter a new method has been reported, and data presented on the motion and inclination angles of the SIJ in two populations of unaffected dogs. This is the first report of an *in vivo* technique to measure SIJ motion in dogs, and is the first report of a method that utilises CT to measure SIJ motion and inclination angles. This study was designed to develop and test an *in vivo* technique utilising CT, for the measurement of the motion and inclination angles of the canine SIJ. The proposed method had low intra-observer variability.

Positioning for the CT scans aimed to achieve the full extent of passive range of motion in flexion and extension. Range of motion was defined as the range of physiological motion. Demoulin et al. (2007) defined passive range of motion as the motion controlled by the passive stabilisation subsystem (in this case made up of the vertebrae, intervertebral disc, ligaments, joint capsules and zygapophyseal joints) and includes motion at the ends of the physiologic range whereby motion is produced against significant resistance (Demoulin et al., 2007). Significant resistance was defined as the resistance at the end of the physiologic range of motion that prevents movement beyond the physiological limit of the tissues. In this present study, the end of the physiological range of extension of the tissues in extension was identified by observation of elevation of the cranial pelvis (analogous to a fulcrum) when the pelvic limbs were extended caudoventrally. In flexion, the end of the physiological range of motion was identified by elevation of the caudal pelvis off the table when the pelvic limbs were pulled cranially. These movements of the pelvis indicated that the physiologic range of motion for the adjacent structures (lumbosacral joint, SIJ, coxofemoral joints) had been

reached. It is not known what effect sedation or anaesthesia may have had on range of motion, but sedation is necessary to perform CT scans on dogs.

The SIJ was found to have very little rotational and translational motion. The main component of translational motion was in the X-axis along the dorsal spinous processes of the sacrum, with very little motion in the Y-axis perpendicular to the dorsal spinous processes. Less motion was measured than has been previously reported in dogs (Gregory et al., 1986). The SIJ is capable of much less motion than the neighbouring higher motion lumbosacral and coxofemoral joints, and the small amount of motion in the SIJ indicates that it is a stiff joint. High frequency vibrations are better absorbed in joints than in a direct bony connection (Tsuchikane et al., 1995). If the sacrum and ilium were instead fused, they would be more efficient at transmitting force during gait, but there is a trade-off between force transmission and buffering. A boney connection may be more susceptible than a joint to degenerative changes due to increased vibration transmission. The buffering of high frequency vibrations by the SIJ may also be important to reduce the amplitude or frequency of vibrations reaching the intervertebral discs.

Increased SIJ rotational motion in GSDs without lumbosacral region pain, as compared to GHs, may be linked to GSDs' predilection for lumbosacral region pain, either directly by causing SIJ pain, or by transferring abnormal loads to adjacent structures such as the lumbosacral joint. Further studies to measure motion in GSDs affected by lumbosacral region pain as compared to unaffected GSDs would assess this potential association. It is important to note that currently our ability to identify and localise pain to the SIJ in dogs is limited and it is possible that the SIJ is unrelated to the development of lumbosacral region pain.

Rotational motion has been previously measured in canine cadavers following soft tissue dissection (Gregory et al., 1986). Our study quantified significantly less rotational motion than what was previously measured in dogs (Gregory et al., 1986). The greater motion previously found could be due to a combination of the removal of soft tissues which play important roles in restricting motion *in vivo*, and potential changes in tissue dynamics following freezing, or through differences in the magnitude of loading forces applied to the joint, and the use of a different methodology to apply the forces.

Although bodyweight had an effect on rotational motion that was nearing significance, the distribution of bodyweights of the dogs varied between the groups. The range of bodyweights in the GSDs was 26-38 kg, while the bodyweights of GHs were clustered between 28-34.5 kg. While the lighter GSDs appeared to have the most rotational motion and the heavier GSDs had less rotational motion, there were no GHs at the higher and lower ends of the GSD weight range which could be used for breed comparisons. Repeating this study with a broader range of bodyweights is needed to examine this effect, and to determine if weight or breed had a significant effect.

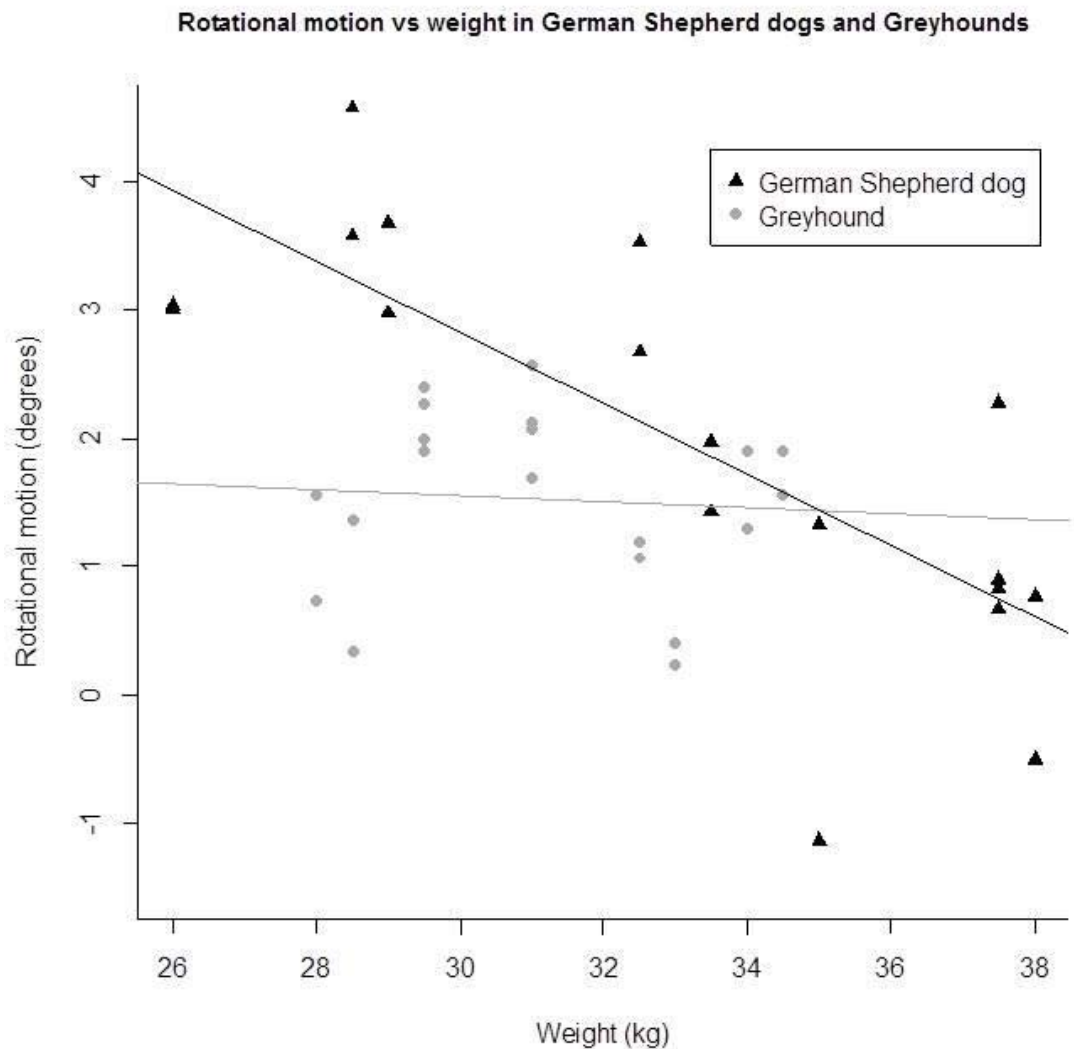


**Figure 2-18 Distribution of average rotational motion vs. weight in German Shepherd dogs and Greyhounds**

The distribution of dog ages varied between the two breeds. The age range of dogs included in this study was deliberately kept narrow in order to minimise the effects of age, and maximise the ability to detect a breed difference. However, the differences in the age distributions between breeds limited the capacity of our model to detect any effect of age. Age was found to have a weak effect on the inclination angle of the cranial synovial component ( $1.5^{\circ}$  for each year) and no significant effect on the remaining variables, but an effect could have been masked by the distribution of ages of the breeds. In addition, it is possible that weight is a confounding variable. There was a moderate association between age and weight in GSDs ( $r=0.59$ ,  $p=0.01$ ) and in GHs ( $r=0.5$ ,  $p=0.02$ ). This study should be repeated with inclusion of a wider range of dog ages to investigate the significance of age on these variables. Further studies are planned to apply this method to a comparison of unaffected GSDs and GSDs affected by lumbosacral region pain.

Sacroiliac joint inclination angles have been previously measured in dogs. Breit et al. (2002) determined inclination angles of the joint by measuring the dorsal and ventral transverse diameters between the sacral wings on radiographs and in cadavers. Direct visualisation of the SIJ space is possible on CT scans, allowing measurement of the axis of the joint space. In some dogs there was a difference between the inclination angles of the ligamentous and synovial components of the SIJ. For this reason, these components were measured separately to create the most accurate measurement of the inclination angles. The cranial synovial component of the SIJ was found to be more sagittally aligned in GSDs than in GHs. No breed differences were found in the other inclination angle components. The significance of the breed difference in the cranial synovial component alone is unknown. It may be that varying SIJ inclination angles have some relationship to the GSD's predilection for developing lumbosacral region pain. Future studies to compare inclination angles between unaffected GSDs and GSDs affected by lumbosacral region pain would provide further information into the involvement of inclination angles in lumbosacral region pain.

It is interesting that no differences were found between the left and right SIJs of the GHs. Repeated unilateral racing leads to asymmetrical adaptive remodeling of the lower limbs. It has been shown that there is a difference in bone mineral density of the central tarsal bone between the left and right pelvic limbs in racing GHs (Thompson et al., 2012). Possible implications of this finding are that either asymmetric forces are not

transferred through the SIJ during racing, or that asymmetric forces do not lead to changes in the joint.

Sacroiliac joint motion was calculated by measuring the change in relative position between two lines that were drawn using arbitrary landmarks that could be clearly identified on both flexed and extended views. The points that were chosen varied between dogs due to anatomical variations and differing scan lengths between dogs, but, as the lines were arbitrarily chosen reference lines, the importance lay in selecting the same points between flexion and extension, rather than between dogs. The coefficients of variance for the motion measurements were between 0.17-1.29% which suggests high accuracy in the ability to recognize the same anatomical landmarks between flexion and extension and thus the appropriateness of this method for measuring motion. In some cases, the intersection point of the ilial and sacral lines was a short distance from the start of the ilial line creating a higher percentage variation in the length of this line. As evident in the low coefficients of variation of the method, this length variation did not have a significant impact on the methodology. As scans which allowed placement of the ilial points further from the intersection point of the ilial and sacral lines produced lower variation in measurements, this could be an improvement in future studies.

The power to identify differences ranged from 0.32-0.41. The power was not strong and it is possible that there may be smaller differences than were able to be detected. But one would have to question whether differences smaller than what were able to be detected would be biologically significant.

A limitation of the study was that inter-observer variability was not assessed. This is an area that would benefit from being assessed in the future.

## **2.5. Conclusion**

In this chapter, a new CT method for the non-invasive *in vivo* measurement of motion and inclination angles of the SIJ in dogs has been presented. These variables were measured in unaffected dogs from two working dog breeds. German Shepherd dogs had increased rotational range of motion relative to GHs. The cranial synovial

component of the SIJ in GSDs was aligned closer to the sagittal plane than in GHs. These breed differences may have a relationship to GSD's predilection to developing lumbosacral region pain, although whether the SIJ is involved in lumbosacral region pain is still unknown. Further studies are planned to measure motion and inclination angles in GSDs that are affected by lumbosacral region pain as a comparison to unaffected GSDs.



## **Chapter Three: Affected dog study**

### **3.1. Introduction**

In Chapter Two, a method was presented for the measurement of the inclination angles and motion of the sacroiliac joint (SIJ) in two working dog breeds (German Shepherd dogs [GSDs] and Greyhounds [GHs]), of which only one breed (the GSD) has a predilection for developing lumbosacral region pain. This method had low intra-observer variability (coefficients of variance ranged from 0.17-1.29% for the motion measurements, and 0.55-2.45% for the inclination angle measurements). The method was assessed on dogs not currently affected by lumbosacral region pain, and it is unknown if these variables are affected by diseases that cause lumbosacral region pain. It was hypothesised that there would be a difference in the SIJ motion and inclination angles between GSDs affected by lumbosacral regional pain, and unaffected GSDs. In this current chapter, the method was applied to affected GSDs and unaffected GSDs, to assess the correlation between the presence of pain and changes in these variables.

Currently, lumbosacral region pain in dogs is largely attributed to diseases of the lumbosacral vertebral facets, lumbosacral intervertebral disc, and coxofemoral joints (Morgan et al., 2000). It is not known if the SIJ is a site of pain in dogs. It is also unknown if the SIJ contributes to diseases of the lumbosacral junction. German Shepherd dogs have a breed predilection for diseases that cause lumbosacral region pain (Schulman and Lippincott, 1988). German Shepherd dogs are commonly used as working police and military dogs (Moore et al., 2001; Evans et al., 2007). These dogs are socially and economically valuable animals, and lumbosacral region pain can be career limiting. The study described in this chapter aimed to investigate the correlation between the presence of pain in the lumbosacral region of GSDs, and the anatomy and biomechanics of the SIJ. Knowledge of variances in the anatomy and biomechanics of the SIJ between affected dogs and unaffected dogs may provide information on the involvement of the SIJ in lumbosacral region pain.

It was hypothesised that there would be differences in the rotational and translational motions of the SIJ, and in the SIJ inclination angles, between GSDs with and without, lumbosacral region pain.

## 3.2. Materials and methods

### 3.2.1. Study group selection

The GSDs without lumbosacral region pain ("unaffected") in this study were the same dogs used in Chapter Two. The GSDs with lumbosacral region pain ("affected") were recruited from clinical cases admitted through the Massey University Veterinary Teaching Hospital. The criteria for inclusion in the affected group for this study were historical abnormalities suggestive of lumbosacral region pain, orthopaedic and neurologic examination findings consistent with the presence of lumbosacral region pain, and evidence of abnormalities of the lumbosacral junction (such as intervertebral disc degeneration and lumbosacral stenosis) on lumbosacral CT scans. Dogs without pain or neurological abnormalities on examination, or CT findings to support the history of lumbosacral region pain were excluded from the affected group of this study. Affected dogs were a combination of retrospective cases gathered from case records and new cases that were recruited for this study. All of the affected dogs presented for decreased ability to work, including the findings of reluctance to jump into vehicles or scale fences, decreased endurance, decreased enthusiasm for attack training, lameness, or displays of pain (e.g. vocalisation). All affected and unaffected dogs underwent the same pelvic limb orthopaedic, and spinal neurological examinations described in the unaffected dog study in Chapter Two. All affected and unaffected dogs were owned by the New Zealand Police Dog section and were either in training or active service.

### 3.2.2. Measurement methodologies

The methodology used in this study for measuring the *in vivo* motion and inclination angles of the SIJ has been described in Chapter Two. This methodology was found to have low coefficients of variance for the measurements of SIJ motion and inclination angles. The variables assessed included the ranges of motion of the ilium relative to the sacrum, and the SIJ inclination angles. Sacroiliac joint ranges of motion were comprised of rotational motion, X-axis translational motion (motion parallel to a line placed along the dorsal spinous processes of the sacrum) and Y-axis translational motion (motion perpendicular to a line placed along the dorsal spinous processes of the sacrum). Inclination angles are defined as the angle of the axis of the joint relative to a dorsally positioned reference line, as measured on transverse plane CT images (Figure

2-1). Sacroiliac joint inclination angles were comprised of the inclination angles of the synovial and ligamentous components as measured at a cranial and caudal location. Anaesthesia, scan positioning and acquisition, motion measurement and calculations, and inclination angle measurements were performed as described in Chapter Two. Measurements were performed in triplicate by a single observer, on CT scans performed on dogs positioned in flexed, extended and neutral positions.

### 3.2.3. Statistical analysis

Differences between the age and weight of the groups were tested using a two-tailed Student's t-test. A mixed linear model that included a random intercepts term for each dog was used to analyse the effects of age, bodyweight, limb, sex and presence of pain on the measurements of rotational motion ( $\phi$ ), translational motions in the X- and Y-axes (dx and dy), the inclination angles, and their interactions. The mixed model adjusted for repeated measures on each dog due to left and right limbs, and was fitted using the restricted maximum likelihood (REML) procedure in R<sup>1</sup>. Differences were considered significant at  $p < 0.05$ . All data were collected in triplicate and results were averaged. All measurements were performed by the same observer with the observer blinded to results from previous trials. Data were tested for normality using the Anderson-Darling test. Outliers from the fitted linear model were identified by examining the plot of standardised residuals against leverage. Identification of outliers was performed using analysis of Cook's distance. Dogs with a Cook's distance of  $>1$  were excluded for that variable. The power to detect a breed difference for each variable was tested using a power calculation for the general linear model and expressed as a probability. Unless otherwise stated, the data are presented as the mean of the three measurements,  $\pm$  standard deviation.

---

<sup>1</sup> R version 15.1, R Foundation for Statistical Computing, Vienna, Austria

### **3.3. Results**

#### **3.3.1. Dogs**

One affected GSD was removed from the study due to the presence of transitional vertebrae in the lumbosacral region. One affected GSD was removed from the study due to insufficient length of the sacrum included in the scan length to allow measurements to be performed. One unaffected GSD was removed from the study due to the presence of transitional vertebrae in the lumbosacral region. This produced a final study number of 9 unaffected GSDs, and 6 affected GSDs. There were 4 female and 5 male unaffected GSDs. All 6 affected GSDs were male. The left SIJ of one unaffected GSD was excluded from the analysis of X- and Y- axis translation due to a high residual Cook's distance, resulting in normally distributed data.

The ages of the unaffected GSDs ranged from 1-6.5 years old, with an average age of 3.25 years. The unaffected dogs ranged in weight from 26-38 kg, with an average weight of 33.1kg. The affected GSDs ranged from 1-7 years old, with an average age of 3.8 years old. The weights of the affected dogs ranged from 31-45 kg with an average of 37.2 kg. There were no significant differences in ages and weights of the groups ( $p>0.15$ ).

History, examination findings and CT findings of the affected dogs are presented in Table 3-1.

**Table 3-1 History, orthopaedic examination, neurologic examination and CT scan findings of the German Shepherd dogs affected by lumbosacral region pain (LS = lumbosacral)**

<b>Dog number</b>	<b>History findings</b>	<b>Orthopaedic and neurologic examination findings</b>	<b>CT scan findings</b>	<b>Diagnosis</b>
1	Difficulty jumping for the last 3 weeks, wide pelvic limb stance, low tail carriage, unwilling to jump, scuffing pelvic limb nails	Limp tail, low slung pelvic limb gait, pain on pressure over LS junction, pain on lordosis of LS junction, pain on pressure over LS epaxial muscles	LS intervertebral disc mineralisation and extrusion causing cauda equina compression, LS instability and L7-S1 intervertebral foraminal stenosis	Degenerative LS stenosis and LS intervertebral disc degeneration and extrusion
2	Acutely weak in pelvic limbs after jumping up at a fence. Off-colour, less energetic, urinating in kennel, scuffing pelvic limb nails infrequently when tired, unwilling to jump and to climb stairs, ataxic when changing direction	Pain on pressure over LS junction, pain on pelvic limb extension, pain on lordosis of LS junction	LS intervertebral disc mineralisation and mild disc prolapse. Extensive spondylosis deformans at the LS junction with enlargement of L7 spinal nerves bilaterally	LS intervertebral disc degeneration and prolapse, and LS spondylosis deformans

3	History of pelvic limb lameness for 2-3 months, intermittently holding up left pelvic limb even at rest but exacerbated by work	Pain on tail jack, questionably repeatable pain on lordosis of LS junction	Mineralisation and protrusion of the LS intervertebral disc. L7-S1 intervertebral foraminal stenosis	Degenerative LS stenosis and dorsal sacral laminar overhang. LS intervertebral disc degeneration and protrusion
4	Lame left pelvic limb for 3 months exacerbated by exercise, dragging left pelvic limb on stairs, scuffing left pelvic limb nails, letting go of arm during arm-training, vocalising with arched back	Low slung pelvic limb gait, pain on coxofemoral joint extension, pain on pressure over LS junction	Dorsal sacral overhang. Mild L7-S1 intervertebral foraminal stenosis with mild conformational compression of L7 spinal nerves bilaterally	Mild degenerative LS stenosis. Dorsal sacral laminar overhang
5	Reluctant to jump, favouring right pelvic limb, scuffing pelvic limb nails, poor arm work, reluctant to climb stairs	Muscle wasting and weakness in pelvic limbs bilaterally, conscious proprioceptive deficits, pain on pressure over LS junction,	Suspicion of L7-S1 right intervertebral foraminal stenosis	Suspected LS stenosis

		scuffing of pelvic limb nails		
6	Reluctant to jump for 4 months, first noticed after falling over	Grade 1/10 lameness at fast gaits, unsteady on pelvic limbs, decreased placing accuracy, difficulty jumping, scuffing of pelvic limb nails, pain on extension of pelvic limbs, mild pain on lordosis of LS junction	Moderate, dynamic LS intervertebral disc prolapse in extension with disc mineralisation. Mild L7 spinal nerve root enlargement	LS intervertebral disc degeneration with mild prolapse, dynamic LS stenosis

### 3.3.2. Motion

Average motion values from the raw data are presented in Table 3-2. Differences between affected and unaffected GSDs were found for rotational and X-axis translational ranges of motion.

Affected GSDs had significantly greater rotational motion than unaffected GSDs ( $p=0.012$ ). Sex had a significant effect on rotational motion ( $p=0.0471$ ), but as there were no female dogs in the affected GSDs group, it cannot be determined if this effect is due to a significant interaction between lumbosacral region pain and sex, or if it is due to the absence of female GSDs from the affected GSD study group. Left vs. right limb, age and bodyweight had no significant effect on rotational motion.

Affected GSDs had more X-axis translational motion than unaffected GSDs ( $p=0.016$ ). There was no effect of age, weight, sex or left vs. right limb on this variable.

There was no significant difference between affected GSDs and non-affected GSDs in Y-axis translational motion ( $p=0.70$ ). There was no effect of age, weight, sex or left vs. right limb on this variable. In order to determine to an 80% likelihood, that there was a genuine difference between breeds of 1.0 mm, a sample size of 52 dogs would be needed.

Model estimates for rotational and X-axis translation motions are presented in Table 3-3.

**Table 3-2 Average values and standard deviations for the rotational and translational motion variables in affected German Shepherd dogs and unaffected German Shepherd dogs (GSD = German Shepherd dog)**

Variable	Mean $\pm$ standard deviation of the raw data	
	Affected GSD	Unaffected GSD
Rotational motion	3.9 $\pm$ 2.4°	2.0 $\pm$ 1.5°
X-axis translational motion	4.0 $\pm$ 3.7 mm	1.0 $\pm$ 0.7 mm
Y-axis translational motion	1.6 $\pm$ 1.8 mm	0.6 $\pm$ 0.4 mm



**Table 3-3 Parameter estimates and their standard errors for the mixed effect linear models of rotational motion, X-axis translational motion and Y-axis translational motion in affected German Shepherd dogs and unaffected German Shepherd dogs (GSD = German Shepherd dog)**

Variable	Estimate	Standard Error	p value
<b>Rotational motion (°)</b>			
Intercept	3.89 <sup>*</sup>	0.69	0.000
GroupUnaffectedGSD	-3.03 <sup>†</sup>	1.03	0.012
SexF	2.52 <sup>‡</sup>	1.14	0.047
<b>X-axis translational motion (mm)</b>			
Intercept	0.40 <sup>§</sup>	0.08	0.000
GroupUnaffectedGSD	-0.31 <sup>  </sup>	0.11	0.016
<b>Y-axis translational motion (mm)</b>			
Intercept	0.16 <sup>¶</sup>	0.04	0.002
GroupUnaffectedGSD	-0.11 <sup>#</sup>	0.05	0.070 (NS)

<sup>\*</sup> Intercept: For a male affected German Shepherd dog, the baseline level for rotational motion is 3.89°

<sup>†</sup> GroupUnaffectedGSD: For a male unaffected German Shepherd dog, the baseline level for rotational motion is 0.86° (3.89-3.03)

<sup>‡</sup> SexF: For a female unaffected German Shepherd dog, rotational motion is 3.38° (= 0.86 + 2.52)

§ Intercept: For an affected German Shepherd dog, the X-axis translational motion is 0.40 mm

|| GroupUnaffectedGSD: For an unaffected German Shepherd dog, the X-axis translational motion is 0.09 mm (= 0.40 - 0.31)

¶ Intercept: For an affected German Shepherd dog, the baseline Y-axis translational motion is 0.16 mm

# GroupUnaffectedGSD: For an unaffected German Shepherd dog, the Y-axis translational motion is 0.05 mm (= 0.16 - 0.11)

### 3.3.3. Inclination angles

The effect of group (affected GSD vs. unaffected GSD) neared statistical significance for the inclination angle of the caudal ligamentous component ( $p=0.052$ ). Weight had a significant effect on rotational motion ( $p=0.042$ ), although the interaction between weight and group was not significant ( $p=0.911$ ). This suggests that the effect of weight was the same for both groups. For every 1 kg increase in bodyweight in affected GSDs, and in unaffected GSDs, there is a decrease in the inclination angle of  $0.32^\circ$ .

There were no differences found between affected GSDs and unaffected GSDs for the inclination angles of the cranial synovial component ( $p=0.796$ ), the cranial ligamentous component ( $p=0.135$ ), and the caudal synovial component ( $p=0.194$ ). There was no effect of age, sex, bodyweight or left vs. right limb on any of these inclination angle variables.

Model estimates for the inclination angle of the caudal ligamentous component are presented in Table 3-4.

.

**Table 3-4 Parameter estimates and their standard errors for the mixed effect linear models of the inclination angle of the caudal ligamentous component in affected German Shepherd dogs and unaffected German Shepherd dogs**

Variable	Estimate	Standard Error	p value
<b>Caudal ligamentous component (°)</b>			
Intercept	96.75 <sup>*</sup>	5.29	0.000
GroupUnaffectedGSD	-2.95 <sup>†</sup>	1.37	0.052 (NS)
Weight	-0.32 <sup>‡</sup>	0.14	0.042

<sup>\*</sup> Intercept: For an affected German Shepherd dog, the baseline inclination angle for the caudal ligamentous component is 96.75°

<sup>†</sup> GroupUnaffectedGSD: For an unaffected German Shepherd dog, the inclination angle for the caudal ligamentous component (°) is 93.8° (= 96.75 - 2.95) in the absence of the effect of weight

<sup>‡</sup> Weight: For every 1 kg increase in bodyweight in affected German Shepherd dogs, and in unaffected German Shepherd dogs, there is a decrease in inclination angle of 0.32°

### 3.4. Discussion

This study applied the methodology described in Chapter Two to compare the motion and inclination angles of the SIJ between GSDs affected by lumbosacral region pain, and GSDs unaffected by lumbosacral region pain. The aim of this study was to investigate the correlation between pain in the lumbosacral region, and the anatomy and biomechanics of the SIJ.

German Shepherd dogs affected by lumbosacral region pain were found to have increased rotational motion (p=0.012) and X-axis translational motion (motion parallel to a line placed along the dorsal spinous processes of the sacrum) (p=0.016) as

compared to unaffected GSDs. It is possible that the increased ranges of motion in affected GSDs as compared to unaffected GSDs may be linked to the presence of lumbosacral region pain. In Chapter Two it was found that unaffected GSDs had increased rotational motion as compared to GHs. These findings might be related to GSDs' predilection for developing diseases that cause lumbosacral region pain. The affected GSDs all had diseases of the lumbosacral junction which included degenerative lumbosacral stenosis, lumbosacral intervertebral disc disease, lumbosacral spondylosis deformans, and dorsal sacral laminar overhang. While causality of the increased SIJ motion in the affected GSDs cannot be determined by this study, four hypotheses can be proposed. Two contrasting hypotheses are proposed regarding causality of disease: firstly, that lumbosacral disease causes increased SIJ motion, and alternatively, that increased SIJ motion causes lumbosacral disease. Two further hypotheses can be formed proposing that lumbosacral diseases and increased SIJ motion are not causatively related.

It may be that diseases of the lumbosacral junction affect the function of the SIJ. The lumbosacral junction is the highest motion joint in the caudal lumbar spine (Benninger et al., 2004). Diseases of the lumbosacral intervertebral disc and surrounding bones (such as lumbosacral spondylosis deformans) may alter motion at the lumbosacral junction (Schmid and Lang, 1993). Forces transmitted between the pelvic limbs and the vertebral column pass through the coxofemoral joints, SIJ and lumbosacral junction (Cook et al., 1996). Altered range of motion of the lumbosacral junction may change the magnitude or direction of the forces transmitted through the SIJ. Alternatively, alterations of the lumbosacral junction may affect the ability of the SIJ to transmit propulsive forces from the pelvic limbs through the lumbosacral junction. These situations could lead to altered forces at the SIJ. Altered magnitude or direction of forces being transmitted through the SIJ could overload the stabilising system of the joint (i.e. the surrounding soft tissues) leading to increased motion or strain, and degenerative changes in the SIJ. It is also possible that lumbosacral disease in the presence of increased SIJ motion in an unaffected SIJ (such as the increased motion present in the GSD breed found in Chapter Two) could predispose the SIJ to overload and degenerative disease. It may be that the increased motion at the SIJ found in unaffected GSDs as compared to GHs is a cause for the GSD's predilection for developing lumbosacral region pain.

An alternative hypothesis is that changes in the SIJ affect the function of the lumbosacral junction. Increased SIJ motion could alter force transfer from the pelvic limbs to the lumbosacral junction, inciting degenerative diseases at the high-motion lumbosacral junction. This hypothesis seems less likely because the SIJ is capable of such small degrees of motion. There was a difference of  $1.9^{\circ}$  of rotational motion, 3 mm of X-axis translational motion and 1mm of Y-axis translational motion found between affected and unaffected GSDs. While these differences are significant in proportion to the total amount of motion that the SIJ is capable of, they are small relative to the  $34.7^{\circ}$  mean flexion-extension range of motion found in the lumbosacral junction of GSDs (Benninger et al., 2004). It seems likely that the lumbosacral junction is able to absorb the slight amounts of increased motion found in the SIJ of affected GSDs, without producing degenerative effects.

The third hypothesis is that this study artificially found an association between lumbosacral region pain and increased SIJ motion due to small sample sizes.

The final hypothesis is that lumbosacral region pain and increased SIJ motion are not related causatively, but that there is some additional factor which independently leads to development of lumbosacral region pain and altered SIJ motion. It may be GSDs have an anatomic propensity for independently developing diseases of both the lumbosacral junction and altered motion of the SIJ. An example is if these dogs have a defect in some factor (i.e. collagen development) that affects development or function of both the lumbosacral junction and SIJ.

There was no difference found between affected GSDs and unaffected GSDs in any of the inclination angles of the SIJ. This suggests that inclination angles of the SIJ do not have an effect on the development of lumbosacral region pain in these dogs. Unaffected GSDs had a more sagittally aligned cranial synovial inclination angle than GHs, but no differences were found in the inclination angles of the other joint components. The significance of one inclination angle component being more sagittal in GSDs than in GHs is uncertain, although it may be that this more sagittal alignment allows the increased rotational motion seen in GSDs, since rotation was measured in the sagittal plane. A study by Breit and Kunzel (2001) found that large breed dogs had more sagittal inclination angles than small breed dogs. That study also found that GSDs had the most sagittal SIJs of any breed. The effect on inclination angles may not be solely

due to size per se, since GSDs were found to be more sagittal than the similarly sized GHs in one SIJ inclination angle component.

This study provided a non-invasive *in vivo* method of measuring the motion and inclination angles of the canine SIJ. It is likely that *in vivo* SIJ motion is different from *in vitro* motion due to the restraining and stabilising effects of soft tissues, and the artificial application of forces to bones during *in vitro* methodologies. Therefore, the development of *in vivo* methodologies is important to give the most accurate representation of SIJ motion. The development of *in vivo* methodologies that can be used in clinical situations is also important.

A limitation of this study was that all the affected GSDs were male. Affected GSDs had significantly greater rotational motion than unaffected GSDs ( $p=0.012$ ), but as there were no female affected GSDs, it cannot be determined if this effect is due to a significant interaction between lumbosacral region pain and sex, or if it is due to the absence of female GSDs from the affected GSD study group. In the unaffected dog study (Chapter Two) there was roughly even sex distribution of both unaffected GSDs and GHs. No effect of sex was found on any of the variables assessed in that study. As there were no female dogs in the affected GSD group, the effect of sex on the development of lumbosacral region pain cannot be assessed. This is a factor that is likely to limit the assessment of the effect of sex on motion and inclination angle variables in working GSDs because the New Zealand Police Dog Section preferentially selects male dogs due to their increased aggression.

Dogs with lumbosacral transitional vertebrae were excluded from this study because transitional vertebrae form asymmetric and abnormal SIJs. Dogs with lumbosacral transitional vertebrae are 8 times more likely to develop cauda equina syndrome than dogs without a lumbosacral transitional vertebra (Flückiger et al., 2006). It is reported that GSDs have a breed predilection for lumbosacral transitional vertebrae (Flückiger et al., 2006). Transitional lumbosacral vertebrae create abnormal morphology of both the sacroiliac joints, and the lumbosacral joint, which may lead to altered LS motion, secondary lumbosacral intervertebral disc degeneration and the increased incidence of cauda equina syndrome. It is likely that transitional vertebrae will affect the motion and inclination angles of the SIJ due to the abnormal joint morphology. Future studies to

measure motion and inclination angles in GSDs with lumbosacral transitional vertebrae would assess this effect.

A limitation of this method is that measurements were performed under sedation or general anaesthesia, in non-weight bearing positions. To be able to state “true” *in vivo* motion, motion would need to be accurately measured in awake, weight-bearing animals during normal gait. No method has been developed that can accurately and non-invasively measure motion under these conditions. Therefore the method used in this study aimed to measure full passive, physiologic range of motion, closely approximating “true” *in vivo* motion (Demoulin et al., 2007). It is felt that this method provides valuable information about the *in vivo* anatomy and biomechanics of the SIJ in GSDs (with and without lumbosacral region pain) and in GHs. Further studies need to be done in dogs with larger sample sizes to more fully assess these variables, and to develop the methodology for a clinical context.

The GSDs included in this study were drawn from the population of GSDs enrolled in the New Zealand Police Dog Section. The study involved small numbers of dogs, and the dogs were all sourced from one population. The small sample sizes are a limitation of this study. Conclusions need to be drawn from the data with awareness of this limitation, and caution should be used when extrapolating these conclusions to other populations of GSDs. This study was designed to develop and test the methodology, and to provide initial information as to the potential importance of SIJ motion and inclination angles in the development of lumbosacral region pain in GSDs. It is hoped that this information will help to direct future research. Further studies incorporating larger sample sizes need to be performed to gather more clinical information about this correlation. Further studies to assess these variables in other populations of GSDs will provide more information about the GSD breed.

It is thought that there are functional relationships between the lumbosacral, coxofemoral and sacroiliac joints. Diseases such as hip dysplasia may affect force transmission through the SIJ due to abnormal coxofemoral function, or due to altered load bearing from pain. The presence or absence of diseases of the coxofemoral joints was not recorded in this current study. Future studies to measure motion and inclination angles of the SIJ in dogs with hip dysplasia and coxofemoral osteoarthritis, would

assess the potential relationship between these joints. Additionally, studies are needed to correlate lumbosacral motion and sacroiliac motion.

It was not possible to determine any causative relationships from this study. It may be that GSDs with conformational diseases that lead to degenerative changes of the lumbosacral junction (such as dorsal sacral overhang, degenerative lumbosacral stenosis and acquired lumbosacral spondylosis deformans) have SIJ motion that is different before undertaking police training, as compared to SIJ motion after several years of intense service. The current study can supply no information as to whether the unaffected GSDs in the study will continue to remain unaffected, or whether they also have some predisposition for developing lumbosacral region pain. Motion of the SIJ measured over a temporal period in a large group of GSDs while concurrently following their training schedule, and clinical situation may provide valuable information as to relationships between diseases of the lumbosacral junction, and SIJ motion. It would be interesting to separate GSDs affected by lumbosacral region pain into groups by diagnosis and investigate if dogs that develop particular diseases are more prone to altered SIJ motion.

The problem still arises that it is unknown if the SIJ is a site of pain in dogs, and if it is, how to localise pain to the joint. It is possible that the development of an effective method of injecting local anaesthetic blocks into the canine SIJ will provide an opportunity to localise pain to the SIJ. Studies to correlate motion with the presence of a positive SIJ block may provide valuable information as to whether changes in motion are linked to SIJ pain.

### **3.5. Conclusion**

In this Chapter, the methodology developed in Chapter Two was applied to a group of GSDs with lumbosacral region pain, as compared to a group of unaffected GSDs. This study was designed to assess for correlations between the presence of lumbosacral region pain and changes in the motion and inclination angles of the SIJ. It was found that affected GSDs had increased rotational, and X-axis translational motions of the SIJ as compared to unaffected GSDs. No differences were found between affected and unaffected GSDs in Y-axis translational motion, or any of the inclination angle



components of the SIJ. It may be that the increased motion of the SIJ in GSDs with lumbosacral region pain is related to the presence of pain. It is possible that diseases of the lumbosacral junction cause changes in motion of the SIJ, or conversely that increased motion at the SIJ leads to diseases of the lumbosacral junction. Alternatively, it may be that the correlations found between increased SIJ motion and the presence of pain were artificial, or that they are independently related without a causative link. It is possible that changes in motion in the SIJ may lead to the development of degenerative changes at the joint. Currently it is not known if the SIJ is a site of pain in dogs, and if it is, how to localise pain to this joint. Further studies need to be done to assess these variables with larger sample sizes.

## Chapter Four: Conclusions

The complex 3-dimensional anatomy and location of the sacroiliac joint (SIJ) in the body make it a difficult joint to study. Studies in dogs have previously been limited to cadavers and ventrodorsal radiographs. The function of the joint has not been confirmed, but is likely to be multifactorial. Sacroiliac joint motion in the dog has previously been measured *in vitro*. Methods have been developed in humans and horses to measure motion *in vivo*, but none of the methods that have been used are both non-invasive and accurate. Canine SIJ inclination angles have previously been measured on symmetrical ventrodorsal pelvic radiographs, and in cadavers. It has been proposed that the transmission of weight is affected by the inclination angle of the SIJ, which may therefore determine the loading capacity of the joint. CT can be used to visualise the canine SIJ, and the cross-sectional properties of CT make it likely to be a valuable tool in assessing this joint. CT has not previously been used to measure motion between the ilium and sacrum, or the inclination angles of the SIJ.

It is possible that the SIJ is an important site of pain in dogs, but as very little is known about the biomechanics of the joint, and how to localise pain to this joint, the importance of the canine SIJ cannot currently be assessed.

This thesis described the development of a non-invasive *in vivo* method to measure the motion and inclination angles of the SIJ in dogs, using CT. In Chapter Two, SIJ motion and inclination angles were measured in two populations of working dogs, which were not currently affected by lumbosacral region pain. Of these two breeds, only one (the German Shepherd dog [GSD]) has a predilection to diseases that cause lumbosacral region pain. It was found that unaffected GSDs had more rotational motion than Greyhounds (GHs), and the cranial synovial joint component was more sagittal than in GHs. There was no difference found between breeds in the other motion and inclination angle variables. This method was found to have low intra-observer variability. It was hypothesised that the increased rotational motion and more sagittal inclination angle in GSDs as compared to GHs may be related to the GSD's predilection for diseases that cause lumbosacral region pain.

In Chapter Three, the method was applied to GSDs with lumbosacral region pain. The affected GSDs had historical abnormalities suggestive of lumbosacral region pain,

orthopaedic and neurologic examination findings consistent with the presence of lumbosacral region pain, and evidence of abnormalities of the lumbosacral junction (such as intervertebral disc degeneration and lumbosacral stenosis) on lumbosacral CT scans. Sacroiliac joint motion and inclination angles were compared between GSDs with, and without lumbosacral pain, to assess for correlations between pain and changes in these variables. It was found that affected GSDs had more rotational motion, and more X-axis translational motion than unaffected GSDs. The difference between affected and unaffected GSDs in Y-axis translational motion neared but did not reach significance. There was no difference between affected and unaffected GSDs in any of the inclination angles of the SIJ. It may be that the increased motion of the SIJ in GSDs with lumbosacral region pain is related to the presence of pain. It is possible that diseases of the lumbosacral junction cause changes in motion of the SIJ, or conversely that increased motion at the SIJ leads to diseases of the lumbosacral junction. Alternatively, it may be that the correlations found between increased SIJ motion and the presence of pain were artificial, or that they are independently related without a causative link. It is possible that changes in motion in the SIJ may lead to the development of degenerative changes at the joint.

Currently, it is not possible to localise pain to the SIJ in dogs. As such, the involvement of the canine SIJ in lumbosacral region pain is unknown. German Shepherd dogs are economically and socially valuable animals used frequently in military and police roles. These dogs are susceptible to lumbosacral region pain which can be career limiting. Future studies which assess these variables in other GSD populations utilising larger sample sizes, assessing information on coxofemoral disease status and the presence of transitional vertebrae, and correlating SIJ motion to lumbosacral motion will provide more information as to the potential clinical importance of this complex joint.

The methodology used in this thesis was found to have low intra-observer variability. This demonstrates its suitability for use in assessing these variables. The method is non-invasive and has the potential to be applied to further clinical patients. A limitation of the motion method is its complexity. The calculations require a good understanding of mathematical principles. This may limit its use by clinicians, unless a tool is developed to allow input of raw data into a calculator allowing quick and accessible calculation of motion.

In conclusion, this thesis presented a new non-invasive *in vivo* method for measuring the motion and inclination angles of the canine SIJ, using CT. Differences in rotational motion and the inclination angle of the cranial synovial component were found between GSDs and GHs that currently did not have lumbosacral region pain. These breed differences may be related to GSDs' predilection for diseases that cause lumbosacral region pain. The method was then applied to GSDs with lumbosacral region pain to assess correlations between the variables and the presence of pain. Differences in motion were found between GSDs with, and without lumbosacral region pain. These differences may be related to the presence of lumbosacral region pain. It is hypothesised that diseases of the lumbosacral junction cause increased SIJ motion. Further studies are needed to assess these variables and investigate this hypothesis.

## References

- Al-Khayer A, Grevitt MP.** (2007). The sacroiliac joint: An underestimated cause for low back pain. *Journal of Back and Musculoskeletal Rehabilitation* 20(4), 135-41
- Benninger MI, Seiler GS, Robinson LE, Ferguson SJ, Bonel HM, Busato AR, Lang J.** (2004). Three-dimensional motion pattern of the caudal lumbar and lumbosacral portions of the vertebral column of dogs. *American Journal of Veterinary Research* 65(5), 544-51
- Bernard TN, Cassidy JD.** (1991). The sacroiliac joint syndrome: Pathophysiology, diagnosis and management. In: Frymoyer JW (ed) *The adult spine: Principles and practice*. Pp 2107-30. Lippincott-Raven Press, New York
- Bogduk N.** (2005). The sacroiliac joint. In: *Clinical anatomy of the lumbar spine and sacrum*. Pp 173-81. Elsevier Limited, Philadelphia
- Breit S, Kunzel W.** (2001). On biomechanical properties of the sacroiliac joint in purebred dogs. *Annals of Anatomy-Anatomischer Anzeiger* 183(2), 145-50
- Breit S, Knaus I, Kunzel W.** (2003). The gross and radiographic appearance of sacroiliac ankylosis capsularis ossea in the dog. *Research in Veterinary Science* 74(1), 85-92
- Breit SM, Knaus IA, Kunzel WWE.** (2002). Use of routine ventrodorsal radiographic views of the pelvis to assess inclination of the wings of the sacrum in dogs. *American Journal of Veterinary Research* 63(9), 1220-5
- Brooke R.** (1924). The sacro-iliac joint. *Journal of Anatomy* 58(4), 299-305
- Bussey MD, Yanai T, Milburn P.** (2004). A non-invasive technique for assessing innominate bone motion. *Clinical Biomechanics* 19(1), 85-90

- Cattley P, Winyard J, Trevaskis J, Eaton S.** (2002). Validity and reliability of clinical tests for the sacroiliac joint. A review of the literature. *Australasian chiropractic & osteopathy* 10(2), 73-80
- Christensen R.** (2011). Plane answers to complex questions: The theory of linear models, 4th edn. Springer Science and Business Media LLC, New York
- Cook JL, Tomlinson JL, Constantinescu GM.** (1996). Pathophysiology, diagnosis, and treatment of canine hip dysplasia. *Compendium on Continuing Education for the Practicing Veterinarian* 18(8), 853-67
- Crawford JT, Manley PA, Adams WM.** (2003). Comparison of computed tomography, tangential view radiography, and conventional radiography in evaluation of canine pelvic trauma. *Veterinary Radiology & Ultrasound* 44(6), 619-28
- Cusi MF.** (2010). Paradigm for assessment and treatment of SIJ mechanical dysfunction. *Journal of bodywork and movement therapies* 14(2), 152-61
- Dalin G, Ekman S, Olsson SE, Jeffcott LB.** (1985). Sacroiliac joints of the horse - normal morphology and findings in suspected chronic joint injuries. *Nordisk Veterinær Medicin* 37(4), 257-8
- Dalin G, Jeffcott LB.** (1986a). Sacroiliac joint of the horse. 1. Gross morphology. *Anatomia Histologia Embryologia-Journal of Veterinary Medicine Series C-Zentralblatt Fur Veterinarmedizin Reihe C* 15(1), 80-94
- Dalin G, Jeffcott LB.** (1986b). Sacroiliac joint of the horse. 2. Morphometric features. *Anatomia Histologia Embryologia-Journal of Veterinary Medicine Series C-Zentralblatt Fur Veterinarmedizin Reihe C* 15(2), 97-107
- Demoulin C, Distree V, Tomasella M, Crielaard JM, Vanderthommen M.** (2007). Lumbar functional instability: A critical appraisal of the literature. *Annales de Readaptation et de Medecine Physique* 50(8), 677-84

- Dontigny RL.** (1985). Function and pathomechanics of the sacroiliac joint - a review. *Physical Therapy* 65(1), 35-44
- Dussault RG, Kaplan PA, Anderson MW.** (2000). Fluoroscopy-guided sacroiliac joint injections. *Radiology* 214(1), 273-7
- Dyson S, Murray R.** (2003). Pain associated with the sacroiliac joint region: A clinical study of 74 horses. *Equine Veterinary Journal* 35(3), 240-5
- Edge-Hughes L.** (2007). Hip and sacroiliac disease: Selected disorders and their management with physical therapy. *Clinical Techniques in Small Animal Practice* 22(4), 183-94
- Egund N, Olsson TH, Schmid H, Selvik G.** (1978). Movements in sacroiliac joints demonstrated with roentgen stereophotogrammetry. *Acta Radiologica-Diagnosis* 19(5), 833-46
- Engeli E, Haussler KK, Erb HN.** (2004). Development and validation of a periarticular injection technique of the sacroiliac joint in horses. *Equine Veterinary Journal* 36(4), 324-30
- Engeli E, Haussler KK.** (2012). Review of injection techniques targeting the sacroiliac region in horses. *Equine Veterinary Education* 24(10), 529-41
- Evans RI, Herbold JR, Bradshaw BS, Moore GE.** (2007). Causes for discharge of military working dogs from service: 268 cases (2000-2004). *Journal of the American Veterinary Medical Association* 231(8), 1215-20
- Faber M, Schamhardt H, Van Weeren R, Barneveld A.** (2001). Methodology and validity of assessing kinematics of the thoracolumbar vertebral column in horses on the basis of skin-fixated markers. *American Journal of Veterinary Research* 62(3), 301-6

- Flückiger MA, Damur-Djuric N, Hässig M, Morgan JP, Steffen F.** (2006). A lumbosacral transitional vertebra in the dog predisposes to cauda equina syndrome. *Veterinary Radiology & Ultrasound* 47(1), 39-44
- Gembardt C.** (1974). Spondylarthropathia deformans der kreuzdarmbeingelenke und ihre beziehung zur spondylopathia deformans des lumbosakralgelenkes. *Berliner und Munchener tierärztliche Wochenschrift* 87(22), 432-7
- Goff L, Van Weeren PR, Jeffcott L, Condie P, McGowan C.** (2010). Quantification of equine sacral and iliac motion during gait: A comparison between motion capture with skin-mounted and bone-fixated sensors. *Equine Veterinary Journal* 42, 468-74
- Goff LM, Jasiewicz J, Jeffcott LB, Condie P, McGowan TW, McGowan CM.** (2006). Movement between the equine ilium and sacrum: In vivo and in vitro studies. *Equine veterinary journal. Supplement* 36, 457-61
- Gregory CR, Cullen JM, Pool R, Vasseur PB.** (1986). The canine sacroiliac joint: Preliminary study of anatomy, histopathology, and biomechanics. *Spine* 11(10), 1044-8
- Indahl A, Kaigle A, Reikeras O, Holm S.** (1999). Sacroiliac joint involvement in activation of the porcine spinal and gluteal musculature. *Journal of Spinal Disorders* 12(4), 325-30
- Jackson RK.** (1975). Diseases of the horse's spine-'comparative aspects'. *Equine Veterinary Journal* 7(2), 79-80
- Jacob HaC, Kissling RO.** (1995). The mobility of the sacroiliac joints in healthy-volunteers between 20 and 50 years of age. *Clinical Biomechanics* 10(7), 352-61
- Jeffcott LB.** (1975). Symposium on back problems in the horse. (2) the diagnosis of diseases of the horse's back. *Equine Veterinary Journal* 7(2), 69-78



- Jeffcott LB, Dalin G, Ekman S, Olsson SE.** (1985). Sacroiliac lesions as a cause of chronic poor performance in competitive horses. *Equine Veterinary Journal* 17(2), 111-8
- Jones JC, Cartee RE, Bartels JE.** (1995). Computed tomographic anatomy of the canine lumbosacral spine. *Veterinary Radiology & Ultrasound* 36(2), 91-9
- Jones JC, Gonzalez LM, Larson MM, Freeman LE, Werre SR.** (2012). Feasibility and accuracy of ultrasound-guided sacroiliac joint injection in dogs. *Veterinary Radiology & Ultrasound* 53(4), 446-54
- Knaus I, Breit S, Kunzel W.** (2003). Appearance of the sacroiliac joint in ventrodorsal radiographs of the normal canine pelvis. *Veterinary Radiology & Ultrasound* 44(2), 148-54
- Knaus I, Breit S, Kunzel W, Mayrhofer E.** (2004). Appearance and incidence of sacroiliac joint disease in ventrodorsal radiographs of the canine pelvis. *Veterinary Radiology & Ultrasound* 45(1), 1-9
- Kunzel W, Breit S, Knaus I.** (2002). Functional interrelations between the lumbosacral, sacroiliac and coxofemoral complex in dogs as denoted by degenerative joint diseases. *Wiener Tierärztliche Monatsschrift* 89(11), 306-11
- Maigne JY, Planchon CA.** (2005). Sacroiliac joint pain after lumbar fusion. A study with anesthetic blocks. *European Spine Journal* 14(7), 654-8
- Mixter WJ, Ayer JB.** (1935). Herniation or rupture of the intervertebral disc into the spinal canal - report of thirty four cases. *New England Journal of Medicine* 213(9), 385-93
- Moore GE, Burkman KD, Carter MN, Peterson MR.** (2001). Causes of death or reasons for euthanasia in military working dogs: 927 cases (1993-1996). *Journal of the American Veterinary Medical Association* 219(2), 209-14

- Morgan JP, Wind A, Davidson AP.** (2000). Lumbosacral disease. In: Morgan JP (ed) *Hereditary bone and joint diseases in the dog*. Pp 209-29. Schlutersche, Hannover, Germany
- Murata Y, Takahashi K, Yamagata M, Takahashi Y, Shimada Y, Moriya H.** (2001). Origin and pathway of sensory nerve fibers to the ventral and dorsal sides of the sacroiliac joint in rats. *Journal of Orthopaedic Research* 19(3), 379-83
- Murphey MD, Wetzel LH, Bramble JM, Levine E, Simpson KM, Lindsley HB.** (1991). Sacroiliitis: Mr imaging findings. *Radiology* 180(1), 239-44
- Rooney JR.** (1977). Sacroiliac arthrosis and "stifle lameness" in the horse. *Modern Veterinary Practice* 58(2), 138-9
- Schmid V, Lang J.** (1993). Measurements on the lumbosacral junction in normal dogs and those with cauda-equina compression. *Journal of Small Animal Practice* 34(9), 437-42
- Schulman AJ, Lippincott CL.** (1988). Canine cauda-equina syndrome. *Compendium on Continuing Education for the Practicing Veterinarian* 10(7), 835-44
- Snijders CJ, Vleeming A, Stoeckart R.** (1993). Transfer of lumbosacral load to iliac bones and legs. 1. Biomechanics of self-bracing of the sacroiliac joints and its significance for treatment and exercise. *Clinical Biomechanics* 8(6), 285-94
- Sturesson B, Selvik G, Uden A.** (1989). Movements of the sacroiliac joints - a roentgen stereophotogrammetric analysis. *Spine* 14(2), 162-5
- Suri S, Gill SE, Massena De Camin S, Wilson D, McWilliams DF, Walsh DA.** (2007). Neurovascular invasion at the osteochondral junction and in osteophytes in osteoarthritis. *Annals of the Rheumatic Diseases* 66(11), 1423-8

- Szadek KM, Hoogland PVJM, Zuurmond WWA, De Lange JJ, Perez RSGM.** (2010). Possible nociceptive structures in the sacroiliac joint cartilage: An immunohistochemical study. *Clinical Anatomy* 23(2), 192-8
- Taylor WR, Ehrig RM, Duda GN, Schell H, Seebeck P, Heller MO.** (2005). On the influence of soft tissue coverage in the determination of bone kinematics using skin markers. *Journal of Orthopaedic Research* 23(4), 726-34
- Thompson D, Cave N, Bridges J, Reuvers K, Owen M, Firth E.** (2012). Bone volume and regional density of the central tarsal bone detected using computed tomography in a cross-sectional study of adult racing greyhounds. *New Zealand veterinary journal* 60(5), 278-84
- Tsuchikane A, Nakatsuchi Y, Nomura A.** (1995). The influence of joints and soft tissue on the natural frequency of the human tibia using the impulse response method. *Proceedings of the Institution of Mechanical Engineers. Part H, Journal of engineering in medicine* 209(3), 149-55
- Tuite MJ.** (2004). Facet joint and sacroiliac joint injection. *Seminars in Roentgenology* 39(1), 37-51
- Vleeming A, Stoeckart R, Volkers ACW, Snijders CJ.** (1990a). Relation between form and function in the sacroiliac joint .1. Clinical anatomical aspects. *Spine* 15(2), 130-2
- Vleeming A, Volkers ACW, Snijders CJ, Stoeckart R.** (1990b). Relation between form and function in the sacroiliac joint .2. Biomechanical aspects. *Spine* 15(2), 133-5
- Worth AJ, Thompson DJ, Hartman AC.** (2009). Degenerative lumbosacral stenosis in working dogs: Current concepts and review. *New Zealand Veterinary Journal* 57(6), 319-30

**Yeoman W.** (1928). The relation of arthritis of the sacro-iliac joint to sciatica, with an analysis of 100 cases. *Lancet* 21, 119-22

**Yu W, Feng F, Dion E, Yang HZ, Jiang M, Genant HK.** (1998). Comparison of radiography, computed tomography and magnetic resonance imaging in the detection of sacroiliitis accompanying ankylosing spondylitis. *Skeletal Radiology* 27(6), 311-20